This is a repository copy of *Underlying-event studies with strange hadrons in pp collisions at √ s = 13 TeV with the ATLAS detector*.

White Rose Research Online URL for this paper:
https://eprints.whiterose.ac.uk/222570/

Version: Published Version

Article:
Aad, G. orcid.org/0000-0002-6665-4934, Aakvaag, E. orcid.org/0000-0001-7616-1554, Abbott, B. orcid.org/0000-0002-5888-2734 et al. (2897 more authors) (2024) Underlying-event studies with strange hadrons in pp collisions at √ s = 13 TeV with the ATLAS detector. The European Physical Journal C, 84 (12). 1335. ISSN 1434-6044

https://doi.org/10.1140/epjc/s10052-024-13243-1

Reuse
This article is distributed under the terms of the Creative Commons Attribution (CC BY) licence. This licence allows you to distribute, remix, tweak, and build upon the work, even commercially, as long as you credit the authors for the original work. More information and the full terms of the licence here: https://creativecommons.org/licenses/

Takedown
If you consider content in White Rose Research Online to be in breach of UK law, please notify us by emailing eprints@whiterose.ac.uk including the URL of the record and the reason for the withdrawal request.

eprints@whiterose.ac.uk
https://eprints.whiterose.ac.uk/

Eur. Phys. J. C (2024) 84:1335
https://doi.org/10.1140/epjc/s10052-024-13243-1

THE EUROPEAN PHYSICAL JOURNAL C

Check for updates

Regular Article - Experimental Physics

Underlying-event studies with strange hadrons in pp collisions at $\sqrt{s} = 13$ TeV with the ATLAS detector

ATLAS Collaboration[⋆]

CERN, 1211 Geneva 23, Switzerland

Received: 9 May 2024 / Accepted: 14 August 2024 / Published online: 29 December 2024
© CERN for the benefit of the ATLAS Collaboration 2024

Abstract Properties of the underlying-event in pp interactions are investigated primarily via the strange hadrons K^0_S, Λ and $\bar{\Lambda}$, as reconstructed using the ATLAS detector at the LHC in minimum-bias pp collision data at $\sqrt{s} = 13$ TeV. The hadrons are reconstructed via the identification of the displaced two-particle vertices corresponding to the decay modes $K^0_S \to \pi^+\pi^-$, $\Lambda \to \pi^- p$ and $\bar{\Lambda} \to \pi^+ \bar{p}$. These are used in the construction of underlying-event observables in azimuthal regions computed relative to the leading charged-particle jet in the event. None of the hadronisation and underlying-event physics models considered can describe the data over the full kinematic range considered. Events with a leading charged-particle jet in the range of $10 < p_T \leq 40$ GeV are studied using the number of prompt charged particles in the transverse region. The ratio $N(\Lambda + \bar{\Lambda})/N(K^0_S)$ as a function of the number of such charged particles varies only slightly over this range. This disagrees with the expectations of some of the considered Monte Carlo models.

Contents

⋆ e-mail: atlas.publications@cern.ch

1 Introduction

The simulation of proton–proton (pp) collisions at the Large Hadron Collider (LHC) is divided into several stages. Typically there is the calculation of a hard interaction in perturbative quantum chromodynamics (QCD), which is followed by QCD-inspired parton shower models and then a phenomenological treatment of the hadronisation of the resulting partons. These hadronisation models, such as the Lund string [1] and cluster [2] models, attempt to act as universal solutions: part of the description of almost all pp collisions. The accuracy of these hadronisation models affects the interpretation of our measurements.

An extra complication is that partons from the pp interaction, in addition to those in the hard scattering, can undergo scattering in a process known as multi-parton interactions (MPI). These additional interactions are typically much softer than the hard interaction which, presumably, triggered the recording of the event.

Typical models of hadronisation have parameters that are tuned using data recorded in e^+e^- collisions from the LEP collider [3,4], as well as from the LHC [5] and other experiments. Much of these data uses the properties of particles identified only as charged hadrons, but K^0_S and $(\Lambda + \bar{\Lambda})$ yields, and properties of strange mesons and baryons in general have also been important in determining these parameters. The parameter sets are known as 'tunes' when applied to models using the Monte Carlo (MC) method and are made public by the experimenters using them. The increasing size of the high-precision LHC datasets demands ever higher precision in the modelling, and motivates an expanded set of measurements to help tune the models. New approaches may also highlight regions where some models do not provide an adequate description.

The mass of the strange quark is close to the divergent scale of perturbative QCD, $\Lambda_{\rm QCD} \sim 250$ MeV, which makes for a subtle interplay between kinematic effects and long-distance (low-energy) QCD interactions. The formation of baryons also presents additional sensitivity to the modelling of MPI

and colour reconnection via the three-way colour junctions required for baryon formation.

This paper presents spectra measurements within individual pp interactions of the strange neutral hadrons K^0_S, Λ and $\bar{\Lambda}$, as measured in low pile-up pp data recorded in 2015 by the ATLAS experiment at the LHC during $\sqrt{s}$= 13 TeV collisions. These strange hadrons are reconstructed in this analysis via their displaced decay vertices, and these particle species are used extensively by LHC experiments to explore hadronisation and fragmentation in hadronic interactions; prior studies include Refs. [6–16].

The $(\Lambda + \bar{\Lambda})$ and K^0_S yields are presented normalised to the total number of events or to the total number of prompt charged-particles, and the relative $(\Lambda + \bar{\Lambda})$ to K^0_S yields are presented in addition. These ATLAS data are compared with MC predictions within a fiducial volume where ATLAS maintains both a high reconstruction efficiency and a low probability of fakes (a mis-reconstructed particle).

Measurements are made following a so called underlying-event (UE) formalism that originated in studies of $p\bar{p}$ collision in CDF [17]; many UE measurements are made based on LHC collision data with different particle species at different centre of mass energies, including ATLAS [18], ALICE [19] and CMS [20].

The charged-particle jet with the highest transverse momentum (p_T) in each event, denoted the 'leading jet', defines an axis in the plane transverse to the beam directions. The azimuth is split into three equal size regions defined by the leading jet as shown in Fig. 1. The towards region contains the $2\pi/3$ of the azimuth centred on the leading jet, the away region is π away and typically contains most hadronic recoil. Finally the transverse region is formed from the two opposite-sided $\Delta\phi \simeq \pm\pi/2$ regions from the leading jet, each of size $\pi/3$. The transverse region is expected to be the most sensitive region in which to study hadronisation effects associated with MPI as it is minimally contaminated by any leading $2 \to 2$ scattering process in the event.

The multiplicity of reconstructed K^0_S, of the combined sum of Λ and $\bar{\Lambda}$, and of prompt charged-particles is measured in each of the towards, transverse and away regions as a function of two variables. First, the multiplicities are measured against the p_T of the leading jet in the event. Second, they are measured against the multiplicity of prompt charged-particles in the transverse region $\left(N_{\mathrm{ch,trans}}\right)$. This variable exhibits sensitivity to per-event MPI fluctuations. This follows from the study performed in Ref. [21] and complements other related measurements such as those performed by ALICE in Refs. [14,15,19,22].

These measurements test a set of fragmentation properties that ATLAS has not previously probed, allowing a range of predictions from different MC models to be compared with data. None of the models considered are entirely satisfactory over the observables, and these data could be used to improve future simulations. Other recent modelling improvements such as the baryonic colour reconnection model integrated into the HERWIG MC generator in Refs. [23,24] are also expected to be sensitive to the results in this paper.

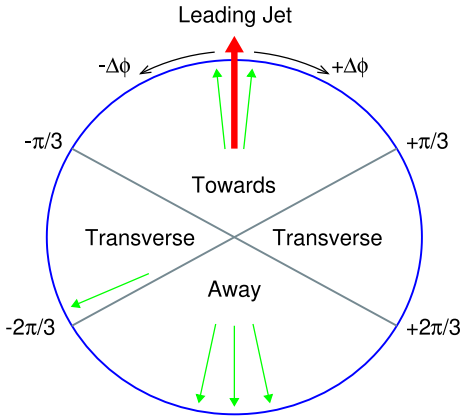

Fig. 1 Illustration of the underlying-event regions relative to the leading jet

The following chapters describe the ATLAS detector (Sect. 2) and the data and simulation samples (Sect. 3). This is followed by the analysis' selections (Sects. 4 and 5), correction factors (Sect. 6), strategy (Sect. 7), uncertainties (Sect. 8), and ends with a set of results as compared with MC models (Sect. 9) and final conclusions (Sect. 10).

2 The ATLAS detector

The ATLAS detector [25] at the LHC covers nearly the entire solid angle around the collision point.[1] It consists of an inner tracking detector surrounded by a thin superconducting solenoid, electromagnetic and hadronic calorimeters, and a muon spectrometer incorporating three large superconducting air-core toroidal magnets. The calorimeter and muon spectrometer detectors are not used by the analysis reported in this paper.

The inner-detector system (ID) is immersed in a 2T axial magnetic field and provides charged-particle tracking in the range $|\eta| < 2.5$. The high-granularity silicon pixel detector covers the vertex region and typically provides four measurements per track, the first hit generally being in the insertable

[1] ATLAS uses a right-handed coordinate system with its origin at the nominal interaction point (IP) in the centre of the detector and the z-axis along the beam pipe. The x-axis points from the IP to the centre of the LHC ring, and the y-axis points upwards. Polar coordinates (r, ϕ) are used in the transverse plane, ϕ being the azimuthal angle around the z-axis. The pseudorapidity is defined in terms of the polar angle θ as $\eta = -\ln\tan(\theta/2)$ and is equal to the rapidity $y = \frac{1}{2}\ln\left(\frac{E+p_z c}{E-p_z c}\right)$ in the relativistic limit. Angular distance is measured in units of $\Delta R \equiv \sqrt{(\Delta y)^2 + (\Delta\phi)^2}$.

B-layer (IBL) installed before Run 2 [26,27]. It is followed by the SemiConductor Tracker (SCT), which usually provides eight measurements per track. These silicon detectors are complemented by the transition radiation tracker (TRT), which enables radially extended track reconstruction up to $|\eta| = 2.0$. The TRT also provides electron identification information based on the fraction of hits (typically 30 in total) above a higher energy-deposit threshold corresponding to transition radiation.

The minimum-bias trigger scintillators (MBTS) [28] provide the trigger signal. These are mounted beyond the inner-detector volume at $z = \pm 3.56$ m and are segmented into two rings in pseudorapidity ($2.07 < |\eta| < 2.76$ and $2.76 < |\eta| < 3.86$), with eight azimuthal sectors in the inner ring and four in the outer.

Inelastic events are selected by the first-level trigger system implemented in custom hardware, followed by selections made by algorithms implemented in software in the high-level trigger [29]. The first-level trigger can accept events from the 40MHz bunch crossings at a rate up to 100kHz, but in the data sample used here it was pre-scaled to run at only about 1.5kHz and all of the events were recorded without additional selection in the high-level trigger.

A software suite [30] is used in data simulation, in the reconstruction and analysis of real and simulated data, in detector operations, and in the trigger and data acquisition systems of the experiment.

3 Data and Monte Carlo samples

Data from six LHC runs as recorded by the ATLAS detector in June 2015 are used. These runs had up to 29 colliding bunches with a large spatial separation between the colliding bunches, and with the probability of an inelastic interaction per bunch crossing being much smaller than one. Only data where the inner detector was operating nominally are included.

For five of the six runs, events were predominately recorded by a single-hemisphere primary trigger that required that at least one MBTS sector was above threshold. For a period during the sixth run, the primary trigger required at least one MBTS sector was above threshold in both the $+z$ and the $-z$ hemispheres of the detector. This two-hemisphere trigger selection introduces a slight bias towards events with a larger number of charged particles over a wider range of pseudorapidity. Events recorded by the two-hemisphere trigger are only used in the second part of the analysis that requires the event's leading jet to be in the range of $10 < p_{\mathrm{T}} \leq 40$ GeV, as described in the following section. There are about 110 M events recorded with the single-hemisphere trigger and an additional 20 M events recorded exclusively with the two-hemisphere trigger.

All triggered events are required to be in coincidence with time windows in which proton bunches were present and colliding in both of the beams in ATLAS. The mean number of inelastic interactions per bunch-crossing, $\langle\mu\rangle$, varied over the runs between $0.003 < \langle\mu\rangle < 0.03$.

Three MC simulation samples are used: EPOS [31] using the EPOS-LHC [32] tune, Pythia8 inelastic [33] with the A2 [34] tune, and Pythia8 inelastic with the Monash tune and modified colour-reconnection model [35] (which was used at particle level only). The ATLAS detector's response to the outputs of the EPOS-LHC and Pythia8 A2 generators was simulated using Geant4 [36,37].

The EPOS MC provides an implementation of a parton-based Gribov–Regge theory [38], which is an effective QCD-inspired field theory describing the hard and soft scattering simultaneously. The treatment of string hadronisation in EPOS is dependent on the local density of string segments per unit volume relative to a critical-density parameter. Each string is classified as being in either a low density coronal region or in a high-density core region. Corona hadronisation proceeds via unmodified string fragmentation whereas the core is subjected to a hydrodynamic evolution, i.e. it is hadronised including additional contributions from longitudinal and radial flow effects [39]. This hydrodynamic collective flow approach to modelling MPI is contrasted against modelling in Pythia8.

Pythia8 inclusive pp non-diffractive events are dominated by t-channel gluon exchange whereas diffractive interactions are modelled via colour-singlet exchange. The modelling in Pythia8 is based on leading-logarithmic initial- and final-state parton showers, a Lund-string hadronisation model, and particle-decays and soft-QCD modelling, in contrast to the hydrodynamic collective flow approach of EPOS. As the partonic cross-section for the t-channel gluon exchange exceeds the hadronic non-diffractive cross-section at low p_{T}, the existence of MPI is implied and included in Pythia8 as an eikonal distribution of perturbative QCD scatterings, governed by impact-parameter and hadronic-overlap functions. The ATLAS minimum-bias tune A2 is used. This tune is based on the MSTW2008 leading order (LO) parton distribution function (PDF) set [40], and was tuned using ATLAS minimum-bias data at 7 TeV for the MPI parameters. It uses Pythia's MPI-based colour reconnection scheme, with mergers of colour flow between MPI systems controlled by a reconnection-range parameter. It provides a good description of both the minimum-bias multiplicity and p_{T} distributions, and transverse energy-flow data [41].

The Monash [42] tune is used in combination with an alternate colour-reconnection model to provide an additional simulation parameterisation which is compared with data. This is latter referred to as Pythia8 Monash+CR (Colour Reconnection). The Monash tune was constructed using Drell–Yan and underlying-event data from ATLAS, but also data from CMS,

from the Super Proton Synchrotron, and from the Tevatron in order to constrain energy scaling. It uses the NNPDF 2.3 LO PDF set [43]. This tune gives an excellent description of the ATLAS 7, 8 and 13 TeVminimum-bias p_{T} spectra [44–46]. Monash is used in conjunction with the 'Mode 2' parameterisation of the colour-reconnection model from Ref. [35]. This model uses approximations to the full group-theoretical weights from SU(3) to compute probabilistic string topologies where short string lengths are favoured. This allows 'string-junction' structures to form, which provides a further source of baryon (and anti-baryon) production. This can arise at larger distances of order five femtometers, as compared with local baryon-production mechanisms.

4 Object selections

The following selections are imposed to identify candidate physics objects using the ATLAS inner-detector.

Prompt tracks: The prompt tracks selection only considers tracks reconstructed from the primary minimum bias tracking step, discussed in more detail in Ref. [47]. This step reconstructs tracks with a maximum transverse impact parameter of 10 mm. Prompt tracks are required to satisfy $p_{\mathrm{T}} > 500\mathrm{MeV}$, $|\eta| < 2.5$, minimum hits requirements in the pixel and SCT, and a χ^2 requirement to remove mismeasured high-p_{T} tracks. Selected tracks are required to have both the transverse and longitudinal (multiplied by $\sin\theta$) absolute impact parameters relative to the primary vertex (see Sect. 5) of less than 1.5 mm. Tracks with $|\eta| < 2.5$ are used as input to jet reconstruction, with a requirement of $|\eta| < 2.1$ being later used to construct underlying-event observables. This minimises contamination from tracks originating from jets with $|\eta| \geq 2.1$.

Jets: The anti$-k_t$algorithm [48,49] with a radius parameter of $R = 0.4$ is used to reconstruct charged-particle jets using the set of prompt tracks as input. The leading jet is defined as the highest-p_{T} jet satisfying $|\eta| < 2.1$; this η restriction prevents edge-effects by ensuring that tracks associated with the jet are all from within the tracking acceptance.

Large-radius tracks: ATLAS' standard tracking is not optimised for the reconstruction of charged particles at large impact parameter; the large-radius tracking runs as a secondary tracking step to improve upon the reconstruction efficiency for these particles. The reconstruction of these tracks is important to maintain efficiency for low-p_{T} charged particles from strange hadron decay which can have large curvature. This secondary step forms tracks with space points that were not used in the primary minimum bias tracking step. The transverse (longitudinal) impact-parameter requirements applied during reconstruction are loosened significantly from 10 to 300 mm (250 to 1500 mm) and the requirement of a pixel hit is dropped. Tracks reconstructed in the large-radius step are not used directly; instead they are supplied as additional inputs to a V^0-finder algorithm.

Table 1 K^0_{S}, Λ and $\bar{\Lambda}$ selection criteria

	K^0_{S}	Λ , $\bar{\Lambda}$
$\lvert\eta\rvert$	< 1.0	< 1.0
p_{T}	> 400 MeV	> 750 MeV
$\cos\theta$	> 0.9990	> 0.9998
R_{xy}	4 mm $< R_{xy} \leq 300$ mm	15 mm $< R_{xy} \leq 300$ mm
$M^{\mathrm{err}}_{V^0}$	< 15 MeV	< 5 MeV
M_{V^0}	$\lvert M_{V^0} - M_{K^0_{\mathrm{S}}}\rvert < 20$ MeV	$\lvert M_{V^0} - M_{\Lambda}\rvert < 7$ MeV

V^0 **finder:** Vertices reconstructed from a pair of oppositely-charged particle tracks are denoted 'V^0'. The V^0-finder algorithm reconstructs candidate two-body decay vertices [8]. The algorithm iterates over all possible pairs of oppositely charged particle tracks in the combined sample of both the primary and the large-radius tracks; no quality selections are applied to the tracks before their use in the V^0 algorithm. The algorithm identifies two-particle vertex candidates with a χ^2 probability $> 1 \times 10^{-4}$. Candidates are rejected if the radius of the innermost space-point on either track is at a smaller radius than the V^0 candidate reconstructed position. The passing V^0 candidates form a preselection sample. They are fitted with each of the $K^0_{\mathrm{S}} \rightarrow \pi^+\pi^-$, $\Lambda \rightarrow p\pi^-$ and $\bar{\Lambda} \rightarrow \bar{p}\pi^+$ particle hypothesis for the positive and negative charged-particle track.

Kaon and Lambda: The selection of K^0_{S}, Λ and $\bar{\Lambda}$ candidates is made from the set of preselected V^0. The selections favour a high-purity sample containing few fake V^0. The selections are listed in Table 1; here θ is the angle in 3D between the direction of the candidate momentum and the line joining the primary and V^0 secondary vertices, R_{xy} is the decay length of the candidate projected on to the x, y plane, M_{V^0} is the candidate's computed mass and $M^{\mathrm{err}}_{V^0}$ is the uncertainty in this mass. Hadron masses are taken as 497.611 ± 0.013 MeV for K^0_{S} and 1115.683 ± 0.006 MeV for Λ and $\bar{\Lambda}$ [50].

Candidates must also satisfy two subsequent cleaning selections. Pairs of selected V^0 of the same species are vetoed if they are less than a distance of $\Delta R < 0.1$ away from each other. This removes duplicate pairs of V^0 that reconstruct from a triplet of tracks. A V^0 is additionally vetoed if it simultaneously satisfies the K^0_{S} and Λ, or K^0_{S} and $\bar{\Lambda}$ selections, which removes ambiguous candidates. It is not possible for a V^0 to simultaneously satisfy the Λ and $\bar{\Lambda}$ selections.

Selected candidates are visualised in an Armenteros–Podolanski diagram [51] in Fig. 2. In this 2D distribution the abscissa is used to plot the asymmetry of the momen-

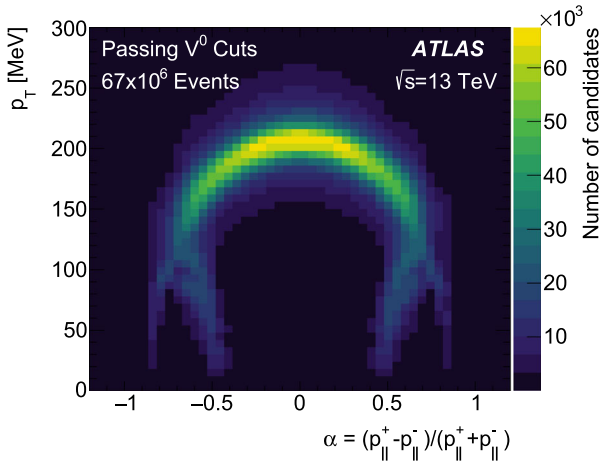

Fig. 2 Armenteros–Podolanski diagram of all K^0_S, Λ and $\bar{\Lambda}$ candidates in data, the ordinate has bin intervals of 6 MeV in p_T and the abscissa has bin intervals of 0.048 in α. See text for the definitions of the ordinate and abscissa

tum component of the V^0's two tracks that is parallel to the V^0's momentum vector, $\alpha = (p^+_\parallel - p^-_\parallel)/(p^+_\parallel + p^-_\parallel)$, and the ordinate to plot the momentum component of the two tracks that is perpendicular to the V^0's momentum vector. K^0_S have symmetric decays and hence a symmetric shape around $\alpha = 0.0$ whereas Λ populate the region near $\alpha = 0.5$ and $\bar{\Lambda}$ the region near $\alpha = -0.5$ as the p (or $\bar{p}$) takes a larger fraction of the decay momentum.

Particle-level selection: The particle level selection defines a fiducial volume, and the data are corrected and unfolded to match this definition. The particle level selection closely follows the reconstruction-level selection. Prompt particles are required to be stable (lifetime $\tau > 0.3 \times 10^{-10}$ s), to not be a charged baryon with lifetime $0.3 \times 10^{-10} < \tau \leq 3.0 \times 10^{-10}$ (see Ref. [47]), $|\eta| < 2.1$ (or $|\eta| < 2.5$, when being used as input to jet finding), have a non-zero charge and $p_T > 500$ MeV.

The reconstruction of charged-particle jets at the particle-level is analogous to the jets selection above at the reconstruction-level.

Branching ratios are folded into the selection of weakly decaying strange hadrons. In addition to the $|\eta|$, p_T and R_{xy} requirements listed above in Table 1, selected K^0_S, Λ and $\bar{\Lambda}$ are required to decay into $\pi^+\pi^-$, $p\pi^-$ and $\bar{p}\pi^+$, respectively. In all cases the two decay-children must satisfy $|\eta| < 2.5$, but there is no explicit p_T requirement on the children. Passing candidates of the same particle species that are less than a distance of $\Delta R < 0.1$ separation are vetoed to mirror the reconstruction-level selections.

5 Event selections

The following requirements are applied to select events for inclusion in the analysis. Physics objects as defined in Sect. 4 are used in the event selection.

Trigger: Data events are required to satisfy the trigger requirements detailed in Sect. 3.

Vertex: Data and MC events are required to contain a primary vertex reconstructed from two or more tracks with $p_T > 100$ MeV following the selection in Ref. [47]. Pile-up events are defined as data events containing two or more reconstructed primary vertices with four or more associated tracks each. These events are removed.

Track: Events are required to have at least one track with $p_T > 1$ GeV which passes the prompt tracking selection. Particle-level events similarly require at least one selected charged particle with $p_T > 1$ GeV.

Jet: Events where the leading jet satisfies $10 < p_T \leq 40$ GeV are classified as having satisfied the restricted leading-jet selection.

A total of 67 M events satisfy the event selections in data, with a 1.4M event subset satisfying the restricted leading-jet selection. The available EPOS-LHC and PYTHIA8 Monash+CR MC statistics are comparable in size to the data, whilst the PYTHIA8 A2 sample is only around 25% of the size of the data.

6 Event and particle correction factors

Some detector effects are corrected for by the application of correction factors. These are applied as an event-level weight for the trigger, and as per-candidate weights for selected tracks and V^0.

Data events selected by the single-hemisphere MBTS trigger are corrected to remove a small trigger inefficiency for low values of leading-jet p_T. This trigger is 98.8% efficient in events with a single track reconstructed relative to the beam spot with $p_T > 500$ MeV, and the efficiency quickly rises to 100% with five or more tracks. No trigger correction is applied to the two-hemisphere MBTS triggered sample due to this only being used in conjunction with a $10 < p_T \leq 40$ GeV requirement on the leading jet, for which the trigger is 100% efficient.

Selected prompt tracks and V^0 are corrected for detector effects by application of a per-track or per-V^0 weight. The initial computation of the weights with MC involves matching the selected prompt tracks and both of the decay tracks of the selected V^0 to particle level tracks. Inner-detector space points are associated with the charged particle that

was found to produce the largest energy deposition. Reconstructed tracks are matched to charged particles based on the fraction of space points on the track that are common to both the reconstructed track and the particle-level particle.

The MC-derived average tracking efficiency for prompt charged pions with $p_{\mathrm{T}} > 500$ MeV is 88% at central pseudorapidity, falling to 75% by $|\eta| = 2.1$. The track-correction weight includes efficiency corrections for charged particles that failed to be reconstructed, and corrections for reconstructed tracks that were not matched to particle level. The correction is assessed as a function of η and p_{T}. Details of the correction are found in Ref. [47].

V^0 are similarly corrected using MC-derived correction factors that are applied on a per-V^0 basis; the details are as follows.

The V^0 correction is factored into an efficiency correction, which is assessed as a function of p_{T} and R_{xy}, and a correction for fakes, which is quantified as a function of p_{T}, R_{xy} and $N_{\mathrm{ch,local}}$. Here $N_{\mathrm{ch,local}}$ counts the number of prompt selected tracks (i.e., from the primary vertex) within a cone of size $\Delta R = 0.2$ around the V^0's momentum vector. It allows the probability of a selected V^0 arising due to combinatorial background or non-prompt strange-hadron production to be assessed as a function of the local charged-particle density. The probability that a Λ candidate is a fake rises from 15% for $N_{\mathrm{ch,local}} = 0$ up to around 50% for $N_{\mathrm{ch,local}} = 6$. The V^0 weight is the product of the efficiency weight ($w_\epsilon = 1/\epsilon$, $w_\epsilon \geq 1$) and the fakes weight ($w_f = 1 - $ fake fraction, $w_f \leq 1$). Examples of the K^0_{S}, Λ and $\bar{\Lambda}$ efficiency and fake distributions are presented in Fig. 3.

The mean correction factor is found by integrating over the fiducial region. The EPOS-LHC reconstruction efficiency is $46.07 \pm 0.01\%$ for K^0_{S}, $30.00 \pm 0.02\%$ for Λ, and $26.20 \pm 0.02\%$ $\bar{\Lambda}$. For comparison, the equivalent efficiency as computed with Pythia8 A2 agrees to within $< 0.01\%$ (0.03%) for K^0_{S}(Λ and $\bar{\Lambda}$). The quoted uncertainties include only the statistical error. The difference between Λ and $\bar{\Lambda}$ is due to the asymmetric momentum distribution in the decay together with the asymmetric efficiency of the ATLAS tracker relative to low-momentum charged-particles. The two MC simulations disagree in the fraction of selected V^0 for which the MC particle record does not contain a strange hadron. This was found to arise from Pythia8 A2 underestimating the inclusive Λ and $\bar{\Lambda}$ yield by up to 50% whereas EPOS-LHC is within 10% of the data. Side-band studies were performed using the functional forms from Ref. [8] to fit the K^0_{S} and $(\Lambda + \bar{\Lambda})$ line-shapes. These studies indicate that data and both of the MC simulations have comparable levels of combinatorial background. The combination of the comparable background with an under predicted yield results in Pythia8 A2 predicting that on average 30% of the reconstructed Λ and $\bar{\Lambda}$ candidates fail to match against a selected particle-level hadron, versus 25% for EPOS-LHC. For K^0_{S} it is around 4% for both of the MC simulations. EPOS-LHC is used to calculate the correction factors applied to the data due to its better agreement with data.

The strange-particle reconstruction efficiency was evaluated under systematically modified ATLAS geometry models derived from the studies in Ref. [52]. The largest effect was observed from a 5% increase in all non-silicon material volumes in the inner detector. The mean efficiency under this geometry model was reduced by 0.7% for K^0_{S} and 0.4% for $(\Lambda + \bar{\Lambda})$, with the largest reduction for V^0 at the low-p_{T} kinematic limit.

Systematic uncertainties are added for both the fake-fraction evaluation via side-bands and efficiency evaluation via material effects in simulation, as discussed in Sect. 8.

7 Analysis strategy

For data and MC simulated events, the leading jet in selected events is used to define the towards, transverse, and away regions of the event. The multiplicity is computed separately in each of these three regions for the selected K^0_{S} candidates, the combined set of $(\Lambda + \bar{\Lambda})$ selected V^0 candidates, and for the selected prompt charged-particles. The per-candidate correction weights from Sect. 6 and Ref. [47] are applied when computing these observables. A further observable 'event count' is added; this observable is used to count the events in each bin of (e.g.) leading-jet p_{T} and therefore allows per-event normalised figures to be formed. Final results are obtained by taking the ratio either between pairs of multiplicity observables, or as a multiplicity observable normalised to the event observable. This normalisation step is performed at the end of the analysis after all events are processed.

Each of the observable's distributions are unfolded before taking these ratios using an iterative method [53,54] with four iterations, after which the process is observed to converge. Simulation from EPOS-LHC is used for the response matrix in the unfolding. The unfolding procedure corrects for migrations between different p_{T} bins of the reconstructed and particle-level leading jet. It does not correct for strange hadron or prompt charged-particle reconstruction effects; these were corrected for by the application of the per-candidate weights incorporated into the observables.

An initial set of results is presented as a function of leading-jet p_{T}. The K^0_{S} and $(\Lambda + \bar{\Lambda})$ multiplicities are normalised to either the prompt charged-particle multiplicity in the same underlying-event region, or to the 'event count' observable to obtain the mean yield.

This analysis strategy is repeated for events satisfying the restricted leading-jet selection, $10 < p_{\mathrm{T}} \leq 40$ GeV. There is less of a dependency on the leading-jet p_{T} in this regime of higher-p_{T} hard-interactions, hence the choice of plot abscissa

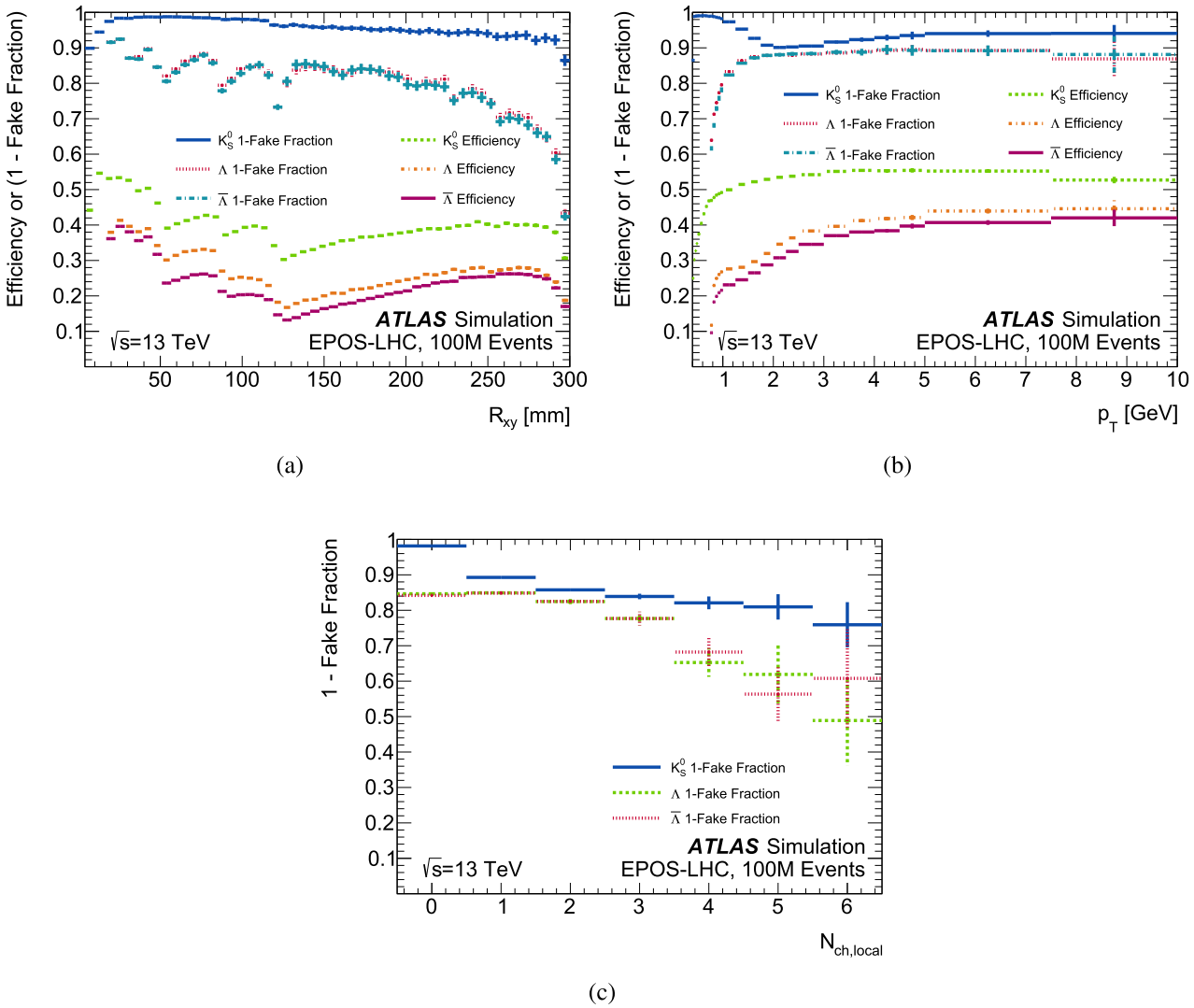

Fig. 3 K^0_S, Λ and $\bar{\Lambda}$ efficiency and (1−fake fraction) as computed from EPOS-LHC MC for **a** R_{xy}, **b** p_T, **c** $N_{ch,local}$. The structure as a function of R_{xy} displayed in **a** is due to the effect of pixel detector layers

is changed to be the multiplicity of prompt charged-particles in the transverse region $(N_{ch,trans})$.

Ratios are presented as a function of $N_{ch,trans}$ for the K^0_S and $(\Lambda + \bar{\Lambda})$ multiplicities normalised to the prompt charged-particle multiplicity in the towards region, and of the relative yield of $(\Lambda + \bar{\Lambda})$ multiplicity to K^0_S multiplicity in the towards and transverse regions.

8 Uncertainties

The following sources of systematic uncertainty are considered. They are assumed to be uncorrelated and are combined in quadrature. Unless noted, the systematic uncertainties are symmetrised around the central value. The unfolding prior, unfolding model, and non-closure systematic uncertainties below are all smoothed with a Gaussian kernel whose width is three times the width of the current bin, to mitigate the effect of statistical fluctuations.

Unfolding prior dependence: The dependence on the MC unfolding prior is evaluated using a reweighting method. The ratio is taken between MC simulation and data for each reconstructed observable and a spline-based interpolation between bins is used to convert this ratio into a weighting function. A reweighted variant of EPOS-LHC acting as pseudo-data is produced. For each event the reweighting function is evaluated based on the particle level leading-jet p_T or $N_{ch,trans}$, the weight is applied to the observable at both the particle and reconstruction levels. The EPOS-LHC pseudo-data are unfolded through the nominal EPOS-LHC response matrix with the nominal number of iterations. The percentage devia-

tion of the unfolded EPOS-LHC pseudo-data with respect of the reweighed EPOS-LHC particle level distribution is taken as a source of uncertainty.

Unfolding model: Data are unfolded through response matrices constructed using the PYTHIA8 A2 MC sample as opposed to the nominal EPOS-LHC MC sample. The per-V^0 correction factors applied to both the data and the PYTHIA8 reconstructed V^0 still wholly originate from EPOS-LHC. This procedure checks for differences between EPOS and PYTHIA8 in the modelling of the leading charged-particle (required to be greater than 1 GeV), the leading jet, and any differences between the modelling of event re-orientation (see below). It also checks against any residual effects from unfolding using a model with a different strange hadron yield, as PYTHIA8 A2's $(\Lambda + \bar{\Lambda})$ yield is significantly smaller than in data. The percentage difference between data unfolded with an EPOS-LHC response matrix and a PYTHIA8 A2 response matrix is taken as a source of uncertainty.

Strange-hadron correction systematic uncertainties: A study was performed in which the probability of selecting a fake V^0 was obtained by fitting the K^0_S, Λ and $\bar{\Lambda}$ line-shapes as discussed in Sect. 6. Inside of the analysis' mass-window, the contribution of the fit associated with combinatorial background differs by a maximum of 2% between the EPOS-LHC MC simulation used to derive the correction factors and the data.

The effect of uncertainty in the material budget of the ATLAS detector model was also included in this systematic via a second study, as additionally discussed in Sect. 6. The efficiency correction factor is modified by a power law that acts to reduce the efficiency by 4% at a V^0 p_{T} of 400 MeV, and increase it by 2%, clamped, for $p_{\mathrm{T}} \geq 8$ GeV.

Both the flat 2% variation in the associated per-V^0 fakes corrections weight and the power-law variation in the per-V^0 efficiency corrections weight are varied independently and included in the strange hadron correction systematic for all of K^0_S, Λ and $\bar{\Lambda}$.

Final contributions in this category are derived from the statistical uncertainty in the evaluation of the efficiency and of the fake fraction. These two components of the V^0 correction weight were independently varied positively and negatively by the respective asymmetric statistical uncertainty.

Prompt-track systematic uncertainties: Systematic uncertainties on prompt tracks from Ref. [47] are included when the multiplicity of prompt tracks is evaluated. This includes the effects of inner-detector material uncertainty, the effect of the χ^2 requirement applied to high-p_{T} tracks, plus an additional flat 0.5% systematic.

Non-closure correction and systematic uncertainty: The EPOS-LHC reconstruction-level observables, including per-particle weighting, are unfolded through the EPOS-LHC response matrices. The term non-closure is used to refer to any residual differences that remain between a reconstruction level MC distribution that was fully corrected for all detector-effects and the corresponding particle level distribution from the same MC sample. Any non-closure is taken both as a correction factor, and as a conservative systematic uncertainty. The application of the correction is integrated into the bootstrap procedure. Many effects can cause this non-closure. Event re-orientation effects are where the ϕ of the leading reconstructed jet does not match the ϕ of the leading particle-level jet. This causes a misalignment of the three underlying-event regions between the particle level and the reconstruction level. The MC modelling of the effect is primarily encoded in the off-diagonal bins of the response matrices as it correlates with a mismatched jet p_{T} between particle level and reconstruction level. Other causes of non-closure effect arise from the V^0 efficiency correction. This correction is computed in bins of particle-level strange hadron kinematics and is then applied on a statistical basis as a correction to the set of reconstructed V^0 candidates.

Two illustrative breakdowns of the systematic uncertainties are shown in addition to the statistical uncertainty and the total uncertainty in Fig. 4, where one breakdown is chosen for each of the two choices of plot abscissa from the following results section. These systematic uncertainties are representative of the final Figs. 5, 6 and 7. All of these figures are obtained from the ratio of two unfolded observables. A bootstrap method [55] is used to obtain the statistical error in each bin. This bootstrap technique uses 500 pseudo-runs in both the data and the MC simulation, each differing as expected across observables due to correlated statistical fluctuations. These correlations are propagated to all of Figs. 4, 5, 6 and 7. The statistical error for each bin in all final figures is taken as the root mean square over all pseudo-runs; the covariance between pairs of bins is computed at the same time.

9 Results

K^0_S and $(\Lambda + \bar{\Lambda})$ multiplicities are presented in Figs. 5 and 6 as a function of the leading-jet p_{T}, with two choices of normalisation. The event-normalised mean distributions show distinct soft and hard regimes, separated by a leading-jet p_{T} of around 10 GeV. The mean values in all distributions show a strong monotonic rise in the soft regime. In the hard regime the mean values either remain constant over the considered range, or continue to rise with a significantly smaller slope. This soft/hard transition is less distinct against the normalisation to the prompt charged-particle yield, here the strange-to-prompt yield is suppressed at low values of leading-jet p_{T} for $(\Lambda + \bar{\Lambda})$ and for K^0_S in the towards region. However for K^0_S in the transverse and away regions it is enhanced. The soft regime is discussed first, followed by the hard regime.

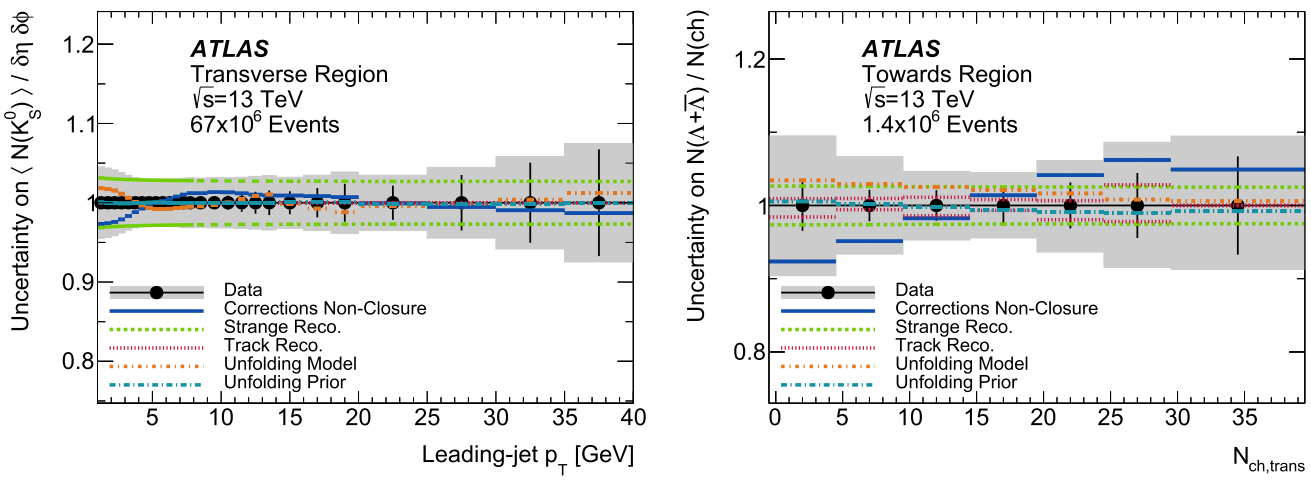

Fig. 4 Breakdown of uncertainties in the measurement of **a** the event-normalised mean number of K^0_S in the transverse region as a function of leading-jet p_T, and **b** for the $(\Lambda + \bar{\Lambda})$ multiplicity as normalised to the prompt charged-particle multiplicity in the towards region as a function of $N_{ch,trans}$. Error bars show the statistical error and the shaded bands show the total uncertainty. The 'Model', 'Prior' and 'Non-closure' systematic uncertainties are symmetrised

No model gives a perfect description of the data, but the EPOS-LHC model gives the best overall performance in the soft regime for both of the choices of normalisation. At a leading-jet p_T of around 5 GeV, EPOS-LHC is observed to correctly model the normalisation for both of the K^0_S and $(\Lambda + \bar{\Lambda})$ mean multiplicities over all underlying-event regions, the agreement is not as good when normalised to prompt charged-particles but EPOS-LHC remains in best or joint-best agreement. At very low leading-jet p_T, EPOS-LHC has a tendency to underestimate, especially for relative baryon yields. Similar and indeed larger trends are observed in the other models. An exception however is the Monash+CR model of the K^0_S and $(\Lambda + \bar{\Lambda})$ relative yields in the towards region, as shown in Figs. 5c, d, 6c, d. The Monash+CR model generally performs as well or better than EPOS-LHC here in the towards region at low leading-jet p_T.

The PYTHIA8 A2 model makes predictions that are significantly too low in all distributions in the soft regime. The underestimation is large in magnitude, up to 40% for the K^0_S distributions in Fig. 5 and up to 60% for the $(\Lambda + \bar{\Lambda})$ distributions in Fig. 6. The PYTHIA8 Monash+CR model performs better than the A2 model for all distributions.

The distributions show a much weaker dependence on the leading-jet p_T in the hard regime. Here the pp interactions are predominately non-diffractive and at low impact parameter; the activity observed is hence driven by a combination of the multiple soft and semi-hard interactions occurring in each event that constitute the underlying-event and the activity from any hard scatter process. The towards and away regions maintain a tendency for the event-normalised mean multiplicity to rise as a function of increasing leading-jet p_T whereas it falls for the prompt-charged normalised cases. The slope is however considerably shallower in the hard regime for both of the choices of normalisation. The transverse region in data is predominately flat over the considered range of the hard regime between $10 < p_T \leq 40$ GeV. This is in part by construction, as this region of the azimuth is minimally affected by any leading partonic $2 \rightarrow 2$ scattering interaction. It is noted that while the event-normalised mean is observed to have only a small dependence on the leading-jet p_T, individual events may show large deviations from the mean, as explored below.

EPOS-LHC does not do as well in the hard regime as it did in the soft regime, likely a consequence of it lacking a hard-scattering model. A common characteristic seen in all event-normalised EPOS-LHC distributions is a decrease in the mean multiplicity above approximately 8 GeV in the leading-jet p_T, and a slower increase above 13 GeV. This deviation from a monotonic rise over the transition from a soft to a hard event structure is not observed in the other considered models, nor would such a dip hypothesis be drawn from the data. After this dip, the EPOS-LHC model predicts a slow monotonic rise in the event normalised yield and slow monotonic fall in the prompt charged-particle normalised yield, the shape of which are generally in good agreement with data. The overall normalisation following the dip region remains too low, however, in the event normalised sample when compared with data. EPOS-LHC under predicts the data by up to 20% in the hard regime.

The PYTHIA8 A2 model performs well in modelling the shape of the distributions in the hard regime. How-

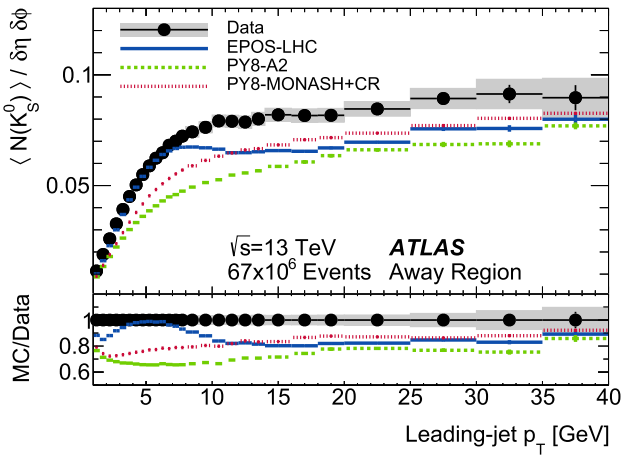

(a)

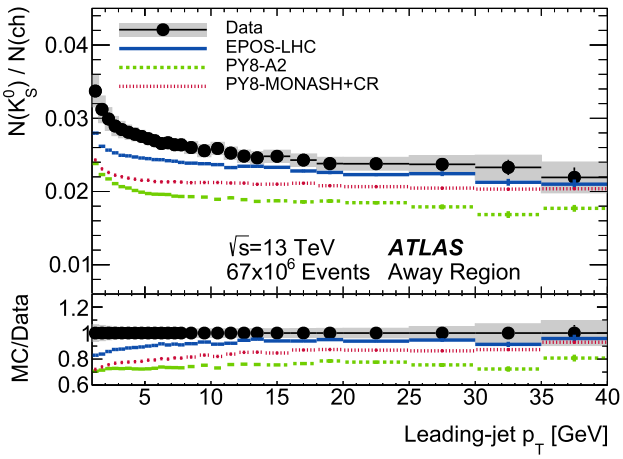

(b)

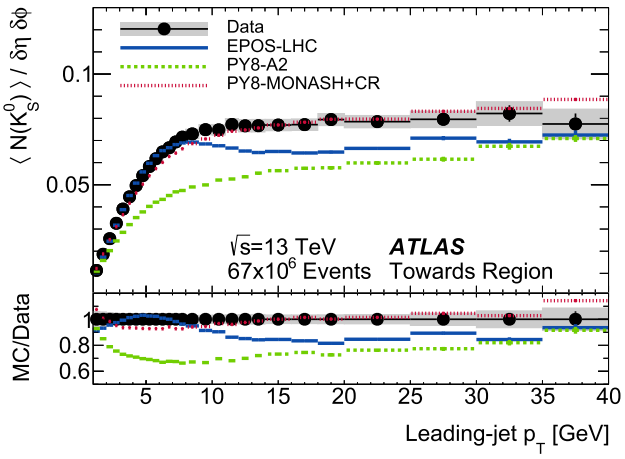

(c)

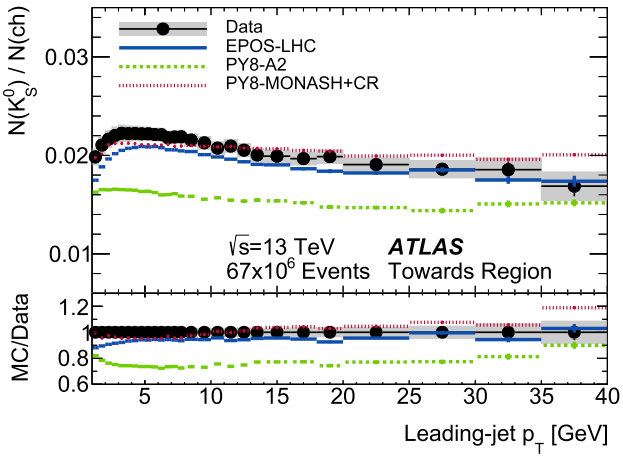

(d)

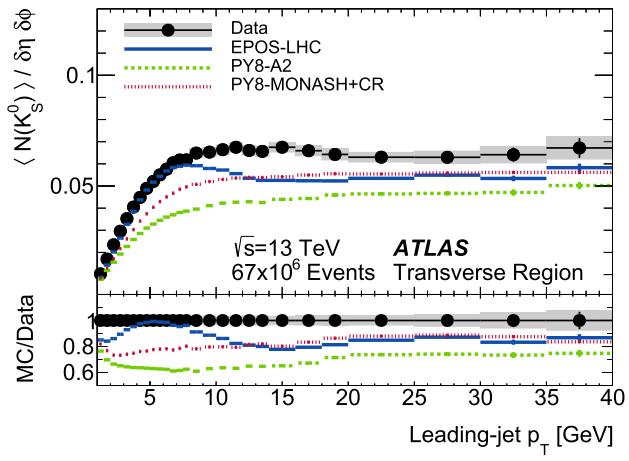

(e)

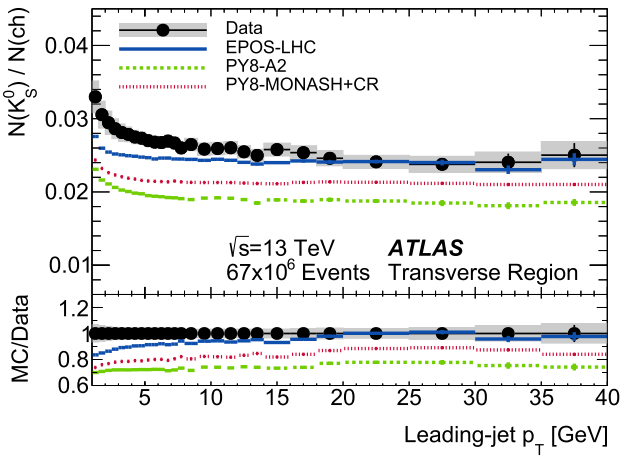

(f)

Fig. 5 (Left) Per event and per unit (η, ϕ) normalised and (right) prompt charged-particle normalised K^0_S yields as a function of leading-jet p_T in the **a** **b** away, **c**, **d** towards and **e**, **f** transverse regions. Error bars show the statistical error and the shaded bands show the combination of statistical and systematic uncertainties

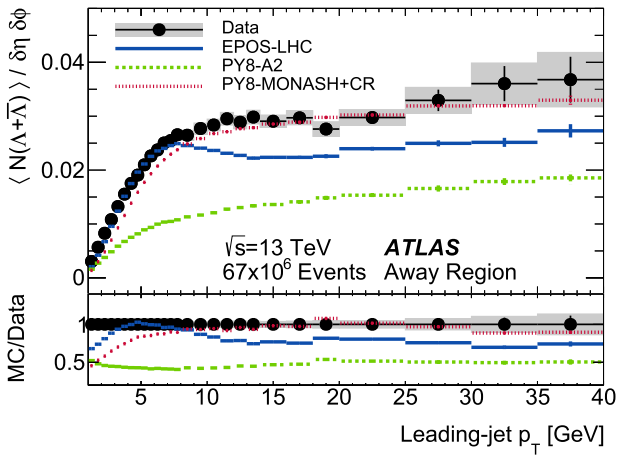

(a)

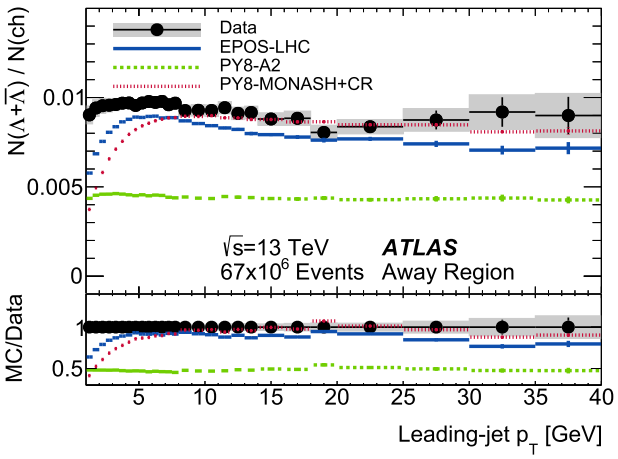

(b)

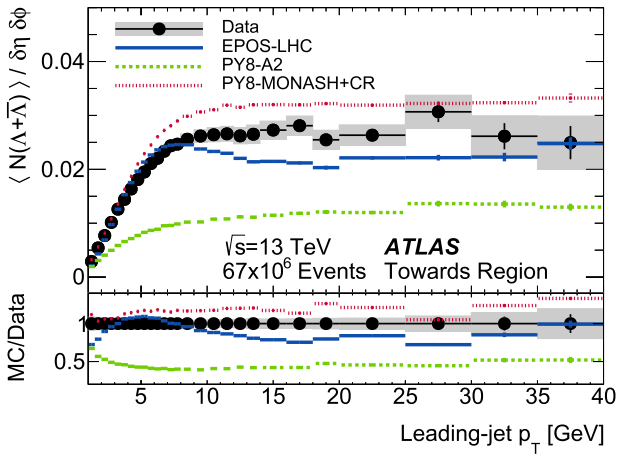

(c)

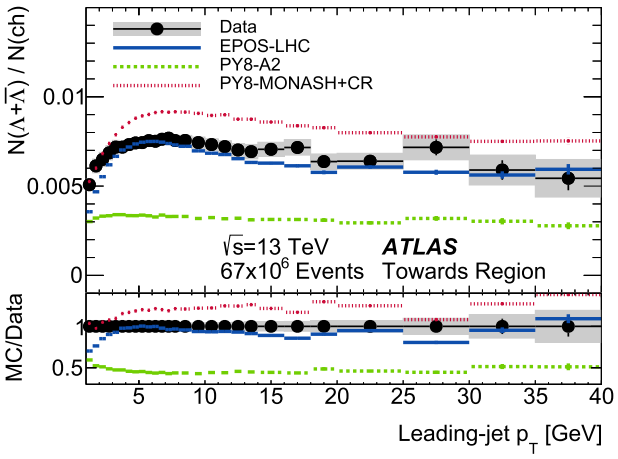

(d)

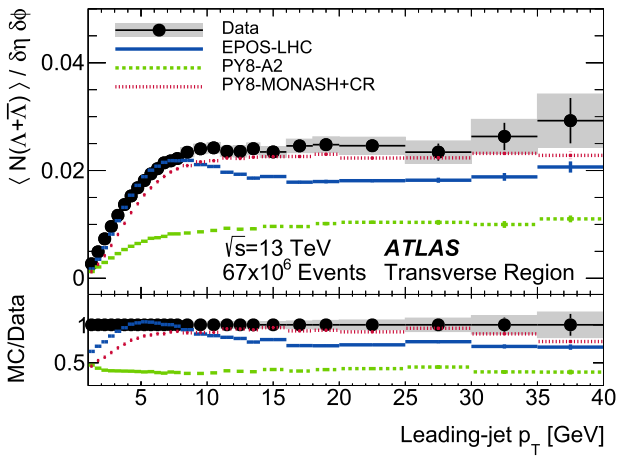

(e)

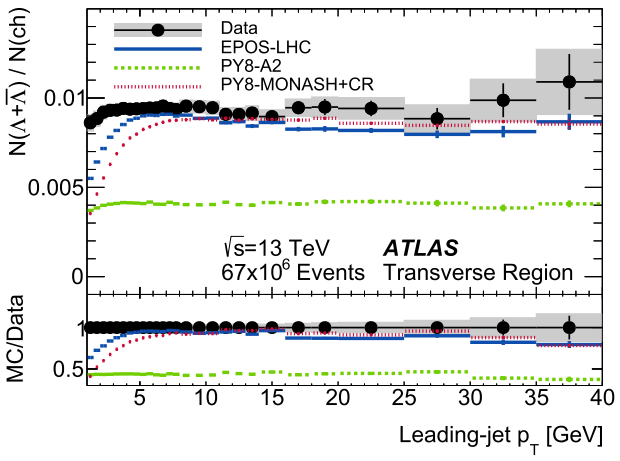

(f)

Fig. 6 (Left) Per event and per unit (η, ϕ) normalised and (right) prompt charged-particle normalised $(\Lambda + \bar{\Lambda})$ yields as a function of leading-jet p_{T} in the **a**, **b** away, **c**, **d** towards and **e**, **f** transverse regions. Error bars show the statistical error and the shaded bands show the combination of statistical and systematic uncertainties

ever, the large under predictions from the soft regime carry forward and the A2 model continues to under predict by 20%–40% for K^0_S distributions, and by 40%–60% for $(\Lambda + \bar{\Lambda})$ distributions for both of the choices of normalisation. The shape of the PYTHIA8 Monash+CR distribution is comparable to A2; however the Monash+CR model is shown to more accurately model an overall higher observed multiplicity in the hard regime. The PYTHIA8 Monash+CR model is observed to be in good agreement with data when modelling the mean multiplicity of K^0_S in the toward region, and of $(\Lambda + \bar{\Lambda})$ in both the away and transverse regions, for both of the choices of normalisation.

For a comparable UE measurement using only prompt charged particles such as Ref. [18], the agreement between data and MC simulation is typically 20% or better, whereas for the strange-particle species in this analysis, differences between data and MC simulation exceeding 50% are observed for some distributions.

The data discussed so far as being in the hard regime are explored further in Fig. 7. The sample of events whose leading jet lies inside $10 < p_{\mathrm{T}} \leq 40$ GeV are included in these figures, with the per-event number of prompt charged-particles in the transverse region $\left(N_{\mathrm{ch,trans}}\right)$ used to define the plot abscissa. $N_{\mathrm{ch,trans}}$ is used as a proxy for the number of soft and semi-hard interactions within the pp collision in this subset of events.

The K^0_S and $(\Lambda + \bar{\Lambda})$ yields as normalised to the charged-particle yield are shown in Fig. 7a, b in the towards region. The model disagreement is worse at small values of $N_{\mathrm{ch,trans}}$ which correspond to events with little activity in the transverse region. EPOS-LHC performs the best here, with the PYTHIA8 A2 model continuing to underestimate the yield while better modelling the shape. The PYTHIA8 Monash+CR model predicts no dependence on the relative K^0_S yield with $N_{\mathrm{ch,trans}}$ in the towards region, which is not in agreement with the data.

In Fig. 7c, d the ratio of $(\Lambda + \bar{\Lambda})$ to K^0_S multiplicity is presented in the towards and transverse regions. The data show only a small suppression of the $(\Lambda + \bar{\Lambda})$ to K^0_S ratio in the towards region for low values of $N_{\mathrm{ch,trans}}$, with the dependence on this ratio in the transverse region as a function of $N_{\mathrm{ch,trans}}$ being even weaker still. Of the considered models, only the more simplistic (with regards to the modelling of strange production in the underlying-event) PYTHIA8 A2 model correctly predicts that the $(\Lambda + \bar{\Lambda})$ to K^0_S ratios are largely insensitive to the $N_{\mathrm{ch,trans}}$ activity levels in the transverse region of the event. However, the absolute value of the ratio from the PYTHIA8 A2 model is under predicted by around 40%, due to the underproduction of $(\Lambda + \bar{\Lambda})$ hadrons in the A2 model relative to data.

These trends may be contrasted with the ALICE measurement in Ref. [14]. A similar enhancement of the strange yield relative to prompt charged-particles is observed by ALICE with respect to prompt charged pions for K^0_S and $(\Lambda + \bar{\Lambda})$. This is seen here in Fig. 7a, b in the towards region of events at higher values of $N_{\mathrm{ch,trans}}$. Here the relative abundance of the strange hadrons is computed in a kinematic space which integrates over all values of leading-jet p_{T} above 10 GeVin order to focus on the scaling of this ratio with the amount of activity in the underlying event, this allows for a more direct probe of colour reconnection effects. This is the opposite scaling trend than what was observed above in Figs. 5d and 6d, where the equivalent strange-particle yields in the towards regions were decreasing as a function of increasing leading-jet p_{T} above 10 GeV. In these distributions the relative abundance of the strange hadrons is integrated over events with small and large levels of underlying event activity and the scaling is more strongly influenced by particle production from jet fragmentation and hadronisation processes at increasingly large momentum scales. This highlights the importance of considering both of the choices of abscissa when investigating the modelling of colour-reconnection effects.

10 Conclusion

Properties of the underlying-event are investigated via the strange hadrons K^0_S, Λ and $\bar{\Lambda}$ in ATLAS minimum-bias pp collision data at $\sqrt{s} = 13$ TeV. The hadrons are reconstructed via the identification of the displaced two-particle vertices corresponding to the decay modes $K^0_S \to \pi^+\pi^-$, $\Lambda \to \pi^- p$ and $\bar{\Lambda} \to \pi^+ \bar{p}$.

K^0_S, Λ and $\bar{\Lambda}$ multiplicity ratios are constructed normalised to the number of events, or to the prompt charged-particle multiplicity in the underlying event 'toward', 'transverse' and 'away' regions relative to the azimuthal angle ϕ of the leading charged-particle jet. They are compared to different MC simulation models.

PYTHIA8 A2 is able to describe the dependence of these observables on the leading-jet p_{T} for both of the K^0_S and $(\Lambda + \bar{\Lambda})$ distributions, but underestimates the yields by around 40%–50%. PYTHIA8 Monash+CR displays an enhanced K^0_S yield and a significantly enhanced $(\Lambda + \bar{\Lambda})$ yield bringing it more in alignment with data. EPOS-LHC is better able to model the rise with leading-jet p_{T}, however it typically plateaus out too early – and even decreases in some event-normalised observables at yet higher leading-jet p_{T}, which is in contrast to what was observed in the data.

A further selection considers events whose leading jet has $10 < p_{\mathrm{T}} \leq 40$ GeV. The Λ/K^0_S ratio is observed to have little dependence of the number of prompt charged-particles in the transverse region, which acts here as a proxy for the number of multi-parton interactions in the event. An enhancement of the K^0_S and $(\Lambda + \bar{\Lambda})$ to prompt charged-particles ratios in the towards region is observed for larger values of the num-

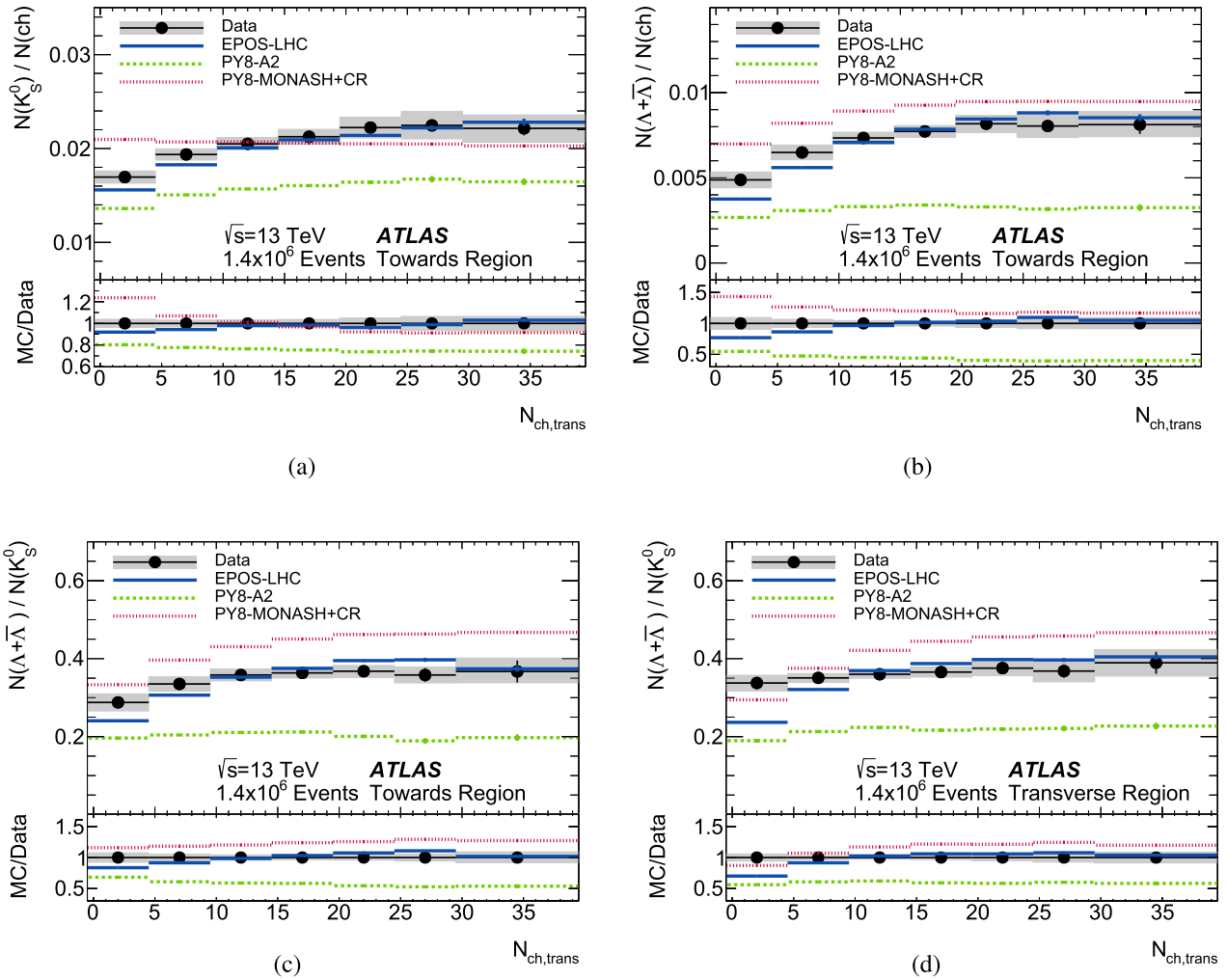

Fig. 7 Comparison between data and MC simulation for several multiplicity ratios as a function of $N_{\mathrm{ch,trans}}$ in events with leading jet $10 < p_{\mathrm{T}} \leq 40$ GeV. Shown are the prompt charged-particle normalised **a** K^0_{S} and **b** $(\Lambda + \bar{\Lambda})$ multiplicity yields in the towards region, and relative yields of $(\Lambda + \bar{\Lambda})$ to K^0_{S} in the **c** towards and **d** transverse regions. Error bars show the statistical error and the shaded bands show the combination of statistical and systematic uncertainties

ber of prompt charged-particles in the transverse region. The EPOS-LHC model is in best agreement with these data.

These data measurements are particularly sensitive to the theoretical modelling and MC tuning of strange and baryon production during hadronisation and may be used to constrain theoretical modelling of non-perturbative effects within individual pp interactions.

Acknowledgements We thank CERN for the very successful operation of the LHC and its injectors, as well as the support staff at CERN and at our institutions worldwide without whom ATLAS could not be operated efficiently. The crucial computing support from all WLCG partners is acknowledged gratefully, in particular from CERN, the ATLAS Tier-1 facilities at TRIUMF/SFU (Canada), NDGF (Denmark, Norway, Sweden), CC-IN2P3 (France), KIT/GridKA (Germany), INFN-CNAF (Italy), NL-T1 (Netherlands), PIC (Spain), RAL (UK) and BNL (USA), the Tier-2 facilities worldwide and large non-WLCG resource providers. Major contributors of computing resources are listed in Ref. [56]. We gratefully acknowledge the support of ANPCyT, Argentina; YerPhI, Armenia; ARC, Australia; BMWFW and FWF, Austria; ANAS, Azerbaijan; CNPq and FAPESP, Brazil; NSERC, NRC and CFI, Canada; CERN; ANID, Chile; CAS, MOST and NSFC, China; Minciencias, Colombia; MEYS CR, Czech Republic; DNRF and DNSRC, Denmark; IN2P3-CNRS and CEA-DRF/IRFU, France; SRNSFG, Georgia; BMBF, HGF and MPG, Germany; GSRI, Greece; RGC and Hong Kong SAR, China; ISF and Benoziyo Center, Israel; INFN, Italy; MEXT and JSPS, Japan; CNRST, Morocco; NWO, Netherlands; RCN, Norway; MNiSW, Poland; FCT, Portugal; MNE/IFA, Romania; MESTD, Serbia; MSSR, Slovakia; ARRS and MIZŠ, Slovenia; DSI/NRF, South Africa; MICINN, Spain; SRC and Wallenberg Foundation, Sweden; SERI, SNSF and Cantons of Bern and Geneva, Switzerland; MOST, Taipei; TENMAK, Türkiye; STFC, United Kingdom; DOE and NSF, United States of America. Individual groups and members have received support from BCKDF, CANARIE, CRC and DRAC, Canada; PRIMUS 21/SCI/017, CERN-CZ and FORTE, Czech Republic; COST, ERC, ERDF, Horizon 2020, ICSC-NextGenerationEU and Marie

Skłodowska-Curie Actions, European Union; Investissements d'Avenir Labex, Investissements d'Avenir Idex and ANR, France; DFG and AvH Foundation, Germany; Herakleitos, Thales and Aristeia programmes co-financed by EU-ESF and the Greek NSRF, Greece; BSF-NSF and MINERVA, Israel; Norwegian Financial Mechanism 2014-2021, Norway; NCN and NAWA, Poland; La Caixa Banking Foundation, CERCA Programme Generalitat de Catalunya and PROMETEO and GenT Programmes Generalitat Valenciana, Spain; Göran Gustafssons Stiftelse, Sweden; The Royal Society and Leverhulme Trust, United Kingdom. In addition, individual members wish to acknowledge support from CERN: European Organization for Nuclear Research (CERN PJAS); Chile: Agencia Nacional de Investigación y Desarrollo (FONDECYT 1190886, FONDECYT 1210400, FONDECYT 1230987); China: National Natural Science Foundation of China (NSFC – 12175119, NSFC 12275265, NSFC-12075060); Czech Republic: Czech Science Foundation (GACR – 24-11373S), Ministry of Education Youth and Sports (FORTE CZ.02.01.01/00/22_008/0004632); European Union: European Research Council (ERC – 948254, ERC 101089007), Horizon 2020 Framework Programme (MUCCA – CHIST-ERA-19-XAI-00), Italian Center for High Performance Computing, Big Data and Quantum Computing (ICSC, NextGenerationEU); France: Agence Nationale de la Recherche (ANR-20-CE31-0013, ANR-21-CE31-0013, ANR-21-CE31-0022), Investissements d'Avenir Labex (ANR-11-LABX-0012); Germany: Baden-Württemberg Stiftung (BW Stiftung-Postdoc Eliteprogramme), Deutsche Forschungsgemeinschaft (DFG – 469666862, DFG – CR 312/5-2); Italy: Istituto Nazionale di Fisica Nucleare (ICSC, NextGenerationEU); Japan: Japan Society for the Promotion of Science (JSPS KAKENHI Grant No. 22KK0227, JSPS KAKENHI JP21H05085, JSPS KAKENHI JP22H01227, JSPS KAKENHI JP22H04944); Netherlands: Netherlands Organisation for Scientific Research (NWO Veni 2020 – VI.Veni.202.179); Norway: Research Council of Norway (RCN-314472); Poland: Polish National Agency for Academic Exchange (PPN/PPO/2020/1/00002/U/00001), Polish National Science Centre (NCN 2021/42/E/ST2/00350, NCN OPUS nr 2022/47/B/ST2/03059, NCN UMO-2019/34/E/ST2/00393, UMO -2020/37/B/ST2/01043, UMO-2021/40/C/ST2/00187, UMO-2022/47/O/ST2/00148, UMO-2023/49/B/ST2/04085); Slovenia: Slovenian Research Agency (ARIS grant J1-3010); Spain: Generalitat Valenciana (Artemisa, FEDER, IDIFEDER/2018/048), Ministry of Science and Innovation (MCIN and NextGenEU – PCI2022-135018-2, MICIN and FEDER – PID2021-125273NB, RYC2019-028510-I, RYC2020-030254-I), PROMETEO and GenT Programmes Generalitat Valenciana (CIDEGENT/2019/023, CIDEGENT/2019/027); Sweden: Swedish Research Council (VR 2018-00482, VR 2022-03845, VR 2022-04683, VR 2023-03403, VR grant 2021-03651), Knut and Alice Wallenberg Foundation (KAW 2018.0157, KAW 2018.0458, KAW 2019.0447, KAW 2022.0358); Switzerland: Swiss National Science Foundation (SNSF - PCEFP2_194658); United Kingdom: Leverhulme Trust (Leverhulme Trust RPG-2020-004), Royal Society (NIF-R1-231091); United States of America: Neubauer Family Foundation.

Data Availability Statement This manuscript has associated data in a data repository. [Authors' comment: The data are available at https://www.hepdata.net/record/ins2784422.]

Code Availability Statement This manuscript has no associated code/software. [Author's comment: Code/Software sharing not applicable to this article as no code/software was generated or analysed during the current study.]

Open Access This article is licensed under a Creative Commons Attribution 4.0 International License, which permits use, sharing, adaptation, distribution and reproduction in any medium or format, as long as you give appropriate credit to the original author(s) and the source, provide a link to the Creative Commons licence, and indicate if changes were made. The images or other third party material in this article are included in the article's Creative Commons licence, unless indicated otherwise in a credit line to the material. If material is not included in the article's Creative Commons licence and your intended use is not permitted by statutory regulation or exceeds the permitted use, you will need to obtain permission directly from the copyright holder. To view a copy of this licence, visit http://creativecommons.org/licenses/by/4.0/.

Funded by SCOAP[3].

References

1. B. Andersson, G. Gustafson, G. Ingelman, T. Sjöstrand, Parton fragmentation and string dynamics. Phys. Rep. **97**, 31 (1983). https://doi.org/10.1016/0370-1573(83)90080-7
2. G. Marchesini et al., HERWIG 5.1—a Monte Carlo event generator for simulating hadron emission reactions with interfering gluons. Comput. Phys. Commun. **67**, 465 (1992). https://doi.org/10.1016/0010-4655(92)90055-4
3. K. Ackerstaff et al., Measurements of flavour-dependent fragmentation functions in $Z^0 \to q\bar{q}$ events. Eur. Phys. J. C **7**, 369 (1999). https://doi.org/10.1007/s100529901067. arXiv:hep-ex/9807004
4. G. Alexander et al., A study of b quark fragmentation into B^0 and B^+ mesons at LEP. Phys. Lett. B **364**, 93 (1995). https://doi.org/10.1016/0370-2693(95)01293-7
5. ATLAS Collaboration, Properties of jet fragmentation using charged particles measured with the ATLAS detector in pp collisions at $\sqrt{s} = 13\ TeV$. Phys. Rev. D **100**, 052011 (2019). https://doi.org/10.1103/PhysRevD.100.052011. arXiv:1906.09254 [hep-ex]
6. CMS Collaboration, Strange particle production in pp collisions at $\sqrt{s} = 0.9$ and 7 TeV. JHEP **05** , 064 (2011). https://doi.org/10.1007/JHEP05(2011)064. arXiv:1102.4282 [hep-ex]
7. CMS Collaboration, Measurement of neutral strange particle production in the underlying event in proton-proton collisions at $\sqrt{s} = 7\ TeV$. Phys. Rev. D **88**, 052001 (2013). https://doi.org/10.1103/PhysRevD.88.052001. arXiv:1305.6016 [hep-ex]
8. ATLAS Collaboration, K^0_S and Λ production in pp interactions at $\sqrt{s} = 0.9$ and 7 TeV measured with the ATLAS detector at the LHC. Phys. Rev. D **85**, 012001 (2012). https://doi.org/10.1103/PhysRevD.85.012001. arXiv:1111.1297 [hep-ex]
9. CMS Collaboration, Observation of sequential Υ suppression in PbPb collisions. Phys. Rev. Lett. **109**, 222301 (2012). https://doi.org/10.1103/PhysRevLett.109.222301. arXiv:1208.2826 [hep-ex]
10. ALICE Collaboration, Multiplicity dependence of (multi-)strange hadron production in proton-proton collisions at $\sqrt{s} = 13\ TeV$. Eur. Phys. J. C **80**, 167 (2020). https://doi.org/10.1140/epjc/s10052-020-7673-8. arXiv:1908.01861 [nucl-ex]
11. ALICE Collaboration, K^0_S - and (anti-)Λ-hadron correlations in pp collisions at $\sqrt{s} = 13\ TeV$. Eur. Phys. J. C **81**, 945 (2021). https://doi.org/10.1140/epjc/s10052-021-09678-5. arXiv:2107.11209 [nucl-ex]
12. ALICE Collaboration, Production of Λ and K^0_S in jets in $p-Pb$ collisions at $\sqrt{s_{NN}} = 5.02$ TeV and pp collisions at $\sqrt{s} = 7$ TeV. Phys. Lett. B **827**, 136984 (2022). arXiv:2105.04890 [nucl-ex]. https://doi.org/10.1016/j.physletb.2022.136984
13. ALICE Collaboration, Production of light-flavor hadrons in pp collisions at $\sqrt{s} = 7$ and $\sqrt{=}13$ TeV. Eur. Phys. J. C **81**, 256 (2021). arXiv:2005.11120 [nucl-ex]. https://doi.org/10.1140/epjc/s10052-020-08690-5
14. ALICE Collaboration, Enhanced production of multi-strange hadrons in high-multiplicity proton-proton collisions. Nat. Phys. **13**, 535 (2017). https://doi.org/10.1038/nphys4111. arXiv:1606.07424 [nucl-ex]

15. ALICE Collaboration, Multiplicity dependence of π, K, and p production in pp collisions at $\sqrt{s} = 13\ TeV$. Eur. Phys. J. C **80**, 693 (2020). https://doi.org/10.1140/epjc/s10052-020-8125-1. arXiv:2003.02394 [nucl-ex]
16. ATLAS Collaboration, Measurement of K^0_S and Λ^0 production in $t\bar{t}$ dileptonic events in pp collisions at $\sqrt{s} = 7$ TeV with the ATLAS detector. Eur. Phys. J. C **79**, 1017 (2019). https://doi.org/10.1140/epjc/s10052-019-7512-y. arXiv:1907.10862 [hep-ex]
17. CDF Collaboration, Underlying event in hard interactions at the Fermilab Tevatron $\bar{p}$p collider. Phys. Rev. D **70**, 072002 (2004). https://doi.org/10.1103/PhysRevD.70.072002
18. ATLAS Collaboration, Measurement of charged-particle distributions sensitive to the underlying event in $\sqrt{s} = 13$ TeV proton-proton collisions with the ATLAS detector at the LHC. JHEP **03**, 157 (2017). https://doi.org/10.1007/JHEP03(2017)157. arXiv:1701.05390 [hep-ex]
19. ALICE Collaboration, Underlying event properties in pp collisions at $\sqrt{s} = 13$ TeV. JHEP **04**, 192 (2020). https://doi.org/10.1007/JHEP04(2020)192. arXiv:1910.14400 [nucl-ex]
20. CMS Collaboration, Measurement of the underlying event in the Drell–Yan process in proton-proton collisions at $\sqrt{s} = 7$ TeV. Eur. Phys. J. C **72**, 2080 (2012). https://doi.org/10.1140/epjc/s10052-012-2080-4. arXiv:1204.1411 [hep-ex]
21. T. Martin, P. Skands, S. Farrington, Probing collective effects in hadronisation with the extremes of the underlying event. Eur. Phys. J. C **76**, 299 (2016). https://doi.org/10.1140/epjc/s10052-016-4135-4. arXiv:1603.05298 [hep-ph]
22. ALICE Collaboration, Measurements of long-range two-particle correlation over a wide pseudorapidity range in $p-Pb$ collisions at $\sqrt{s_{NN}} = 5.02$ TeV. JHEP **01**, 199 (2024). https://doi.org/10.1007/JHEP01(2024)199. arXiv:2310.07490 [nucl-ex]
23. J. Bellm et al., Herwig 7.2 release note. Eur. Phys. J. C **80**, 452 (2020). https://doi.org/10.1140/epjc/s10052-020-8011-x. arXiv:1912.06509 [hep-ph]
24. S. Gieseke, P. Kirchgaeßer, S. Plätzer, Baryon production from cluster hadronisation. Eur. Phys. J. C **78**, 99 (2018). https://doi.org/10.1140/epjc/s10052-018-5585-7. arXiv:1710.10906 [hep-ph]
25. ATLAS Collaboration, The ATLAS experiment at the CERN large hadron collider. JINST **3**, S08003 (2008). https://doi.org/10.1088/1748-0221/3/08/S08003
26. ATLAS Collaboration, ATLAS Insertable B-Layer: Technical Design Report, ATLAS-TDR-19; CERN-LHCC-2010-013 (2010). https://cds.cern.ch/record/1291633 [Addendum: ATLAS-TDR-19-ADD-1; CERN-LHCC-2012-009, 2012, https://cds.cern.ch/record/1451888]
27. B. Abbott et al., Production and integration of the ATLAS Insertable B-Layer. JINST **13**, T05008 (2018). https://doi.org/10.1088/1748-0221/13/05/T05008. arXiv: 1803.00844 [physics.ins-det]
28. ATLAS Collaboration, Performance of the minimum bias trigger in p p collisions at$\sqrt{s} = 7$ TeV, ATLAS-CONF-2010-068 (2010). https://cds.cern.ch/record/1281343
29. ATLAS Collaboration, Performance of the ATLAS trigger system in 2015. Eur. Phys. J. C **77**, 317 (2017). https://doi.org/10.1140/epjc/s10052-017-4852-3. arXiv:1611.09661 [hep-ex]
30. ATLAS Collaboration, Software and computing for Run 3 of the ATLAS experiment at the LHC (2024). arXiv:2404.06335 [hep-ex]
31. T. Pierog, K. Werner, EPOS model and ultra high energy cosmic rays. Nucl. Phys. B Proc. Suppl. **196**, 102 (2009). https://doi.org/10.1016/j.nuclphysbps.2009.09.017. arXiv:0905.1198 [hep-ph]
32. T. Pierog, I. Karpenko, J.M. Katzy, E. Yatsenko, K. Werner, EPOS LHC: test of collective hadronization with data measured at the CERN large hadron collider. Phys. Rev. C **92**, 034906 (2015). https://doi.org/10.1103/PhysRevC.92.034906. arXiv:1306.0121 [hep-ph]
33. T. Sjöstrand et al., An introduction to PYTHIA 8.2. Comput. Phys. Commun. **191**, 159 (2015). https://doi.org/10.1016/j.cpc.2015.01.024. arXiv:1410.3012 [hep-ph]
34. ATLAS Collaboration, Further ATLAS tunes of PYTHIA 6 and Pythia 8, ATL-PHYS-PUB-2011-014 (2011). https://cds.cern.ch/record/1400677
35. J.R. Christiansen, P.Z. Skands, String formation beyond leading colour. JHEP **08**, 003 (2015). https://doi.org/10.1007/JHEP08(2015)003. arXiv:1505.01681 [hep-ph]
36. S. Agostinelli et al., Geant4, a simulation toolkit. Nucl. Instrum. Meth. A **506**, 250 (2003). https://doi.org/10.1016/S0168-9002(03)01368-8
37. ATLAS Collaboration, The ATLAS simulation infrastructure. Eur. Phys. J. C **70**, 823 (2010). https://doi.org/10.1140/epjc/s10052-010-1429-9. arXiv:1005.4568 [physics.ins-det]
38. H.J. Drescher, M. Hladik, S. Ostapchenko, T. Pierog, K. Werner, Parton-based Gribov–Regge theory. Phys. Rep. **350**, 93 (2001). https://doi.org/10.1016/S0370-1573(00)00122-8. arXiv:hep-ph/0007198
39. K. Werner, Core-corona separation in ultra-relativistic heavy ion collisions. Phys. Rev. Lett. **98**, 152301 (2007). https://doi.org/10.1103/PhysRevLett.98.152301. arXiv:0704.1270 [nucl-th]
40. A.D. Martin, W.J. Stirling, R.S. Thorne, G. Watt, Parton distributions for the LHC. Eur. Phys. J. C **63**, 189 (2009). https://doi.org/10.1140/epjc/s10052-009-1072-5. arXiv:0901.0002 [hep-ph]
41. ATLAS Collaboration, Measurements of the pseudorapidity dependence of the total transverse energy in proton-proton collisions at $\sqrt{s} = 7\ TeV$ with ATLAS. JHEP **11**, 033 (2012). https://doi.org/10.1007/JHEP11(2012)033. arXiv:1208.6256 [hep-ex]
42. P. Skands, S. Carrazza, J. Rojo, Tuning PYTHIA 8.1: the Monash 2013 Tune. Eur. Phys. J. C **74**, 3024 (2014). https://doi.org/10.1140/epjc/s10052-014-3024-y. arXiv:1404.5630 [hep-ph]
43. NNPDF Collaboration, R.D. Ball et al., Parton distributions with LHC data. Nucl. Phys. B **867**, 244 (2013). https://doi.org/10.1016/j.nuclphysb.2012.10.003. arXiv:1207.1303 [hep-ph]
44. ATLAS Collaboration, Charged-particle distributions in $\sqrt{s} = 13$ TeV p p interactions measured with the ATLAS detector at the LHC. Phys. Lett. B **758**, 67 (2016). https://doi.org/10.1016/j.physletb.2016.04.050. arXiv:1602.01633 [hep-ex]
45. ATLAS Collaboration, Charged-particle multiplicities in pp interactions measured with the ATLAS detector at the LHC. New J. Phys. **13**, 053033 (2011). https://doi.org/10.1088/1367-2630/13/5/053033. arXiv:1012.5104 [hep-ex]
46. ATLAS Collaboration, Charged-particle distributions in pp interactions at $\sqrt{s} = 8$ TeV measured with the ATLAS detector. Eur. Phys. J. C **76**, 403 (2016). https://doi.org/10.1140/epjc/s10052-016-4203-9. arXiv:1603.02439 [hep-ex]
47. ATLAS Collaboration, Charged-particle distributions at low transverse momentum in $\sqrt{s} = 13$ TeV pp interactions measured with the ATLAS detector at the LHC. Eur. Phys. J. C **76**, 502 (2016). https://doi.org/10.1140/epjc/s10052-016-4335-y. arXiv:1606.01133 [hep-ex]
48. M. Cacciari, G. P. Salam, G. Soyez, The $anti-k_t$ jet clustering algorithm. JHEP **04**, 063 (2008). https://doi.org/10.1088/1126-6708/2008/04/063. arXiv:0802.1189 [hep-ph]
49. M. Cacciari, G.P. Salam, G. Soyez, FastJet user manual. Eur. Phys. J. C **72**, 1896 (2012). https://doi.org/10.1140/epjc/s10052-012-1896-2. arXiv:1111.6097 [hep-ph]
50. P.A. Zyla et al., Review of particle physics. PTEP **2020**, 083C01 (2020). https://doi.org/10.1093/ptep/ptaa104
51. J. Podolanski, R. Armenteros III., Analysis of V-events. Lond. Edinb. Dubl. Philos. Mag. **45**, 13 (1954)
52. ATLAS Collaboration, Studies of the ATLAS inner detector material using $\sqrt{s} = 13$ TeV pp collision data, ATL-PHYS-PUB-2015-050 (2015). https://cds.cern.ch/record/2109010

53. G. D'Agostini, A multidimensional unfolding method based on Bayes' theorem. Nucl. Instrum. Meth. A **362**, 487 (1995). https://doi.org/10.1016/0168-9002(95)00274-X
54. T. Adye, Unfolding algorithms and tests using RooUnfold. In *Proceedings, 2011 Workshop on Statistical Issues Related to Discovery Claims in Search Experiments and Unfolding (PHYSTAT 2011)* (CERN, Geneva, 17th–20th Jan. 2011), 313. arXiv:1105.1160 [physics.data-an]
55. ATLAS Collaboration, Evaluating statistical uncertainties and correlations using the bootstrap method, ATL-PHYS-PUB-2021-011 (2021). https://cds.cern.ch/record/2759945
56. ATLAS Collaboration, ATLAS Computing Acknowledgements, ATL-SOFT-PUB-2023-001 (2023). https://cds.cern.ch/record/2869272

ATLAS Collaboration*

G. Aad[103], E. Aakvaag[16], B. Abbott[121], S. Abdelhameed[117a], K. Abeling[55], N. J. Abicht[49], S. H. Abidi[29], M. Aboelela[44], A. Aboulhorma[35e], H. Abramowicz[152], H. Abreu[151], Y. Abulaiti[118], B. S. Acharya[69a,69b,k], A. Ackermann[63a], C. Adam Bourdarios[4], L. Adamczyk[86a], S. V. Addepalli[26], M. J. Addison[102], J. Adelman[116], A. Adiguzel[21c], T. Adye[135], A. A. Affolder[137], Y. Afik[39], M. N. Agaras[13], J. Agarwala[73a,73b], A. Aggarwal[101], C. Agheorghiesei[27c], A. Ahmad[36], F. Ahmadov[38,y], W. S. Ahmed[105], S. Ahuja[96], X. Ai[62e], G. Aielli[76a,76b], A. Aikot[164], M. Ait Tamlihat[35e], B. Aitbenchikh[35a], M. Akbiyik[101], T. P. A. Åkesson[99], A. V. Akimov[37], D. Akiyama[169], N. N. Akolkar[24], S. Aktas[21a], K. Al Khoury[41], G. L. Alberghi[23b], J. Albert[166], P. Albicocco[53], G. L. Albouy[60], S. Alderweireldt[52], Z. L. Alegria[122], M. Aleksa[36], I. N. Aleksandrov[38], C. Alexa[27b], T. Alexopoulos[10], F. Alfonsi[23b], M. Algren[56], M. Alhroob[168], B. Ali[133], H. M. J. Ali[92], S. Ali[31], S. W. Alibocus[93], M. Aliev[33c], G. Alimonti[71a], W. Alkakhi[55], C. Allaire[66], B. M. M. Allbrooke[147], J. F. Allen[52], C. A. Allendes Flores[138f], P. P. Allport[20], A. Aloisio[72a,72b], F. Alonso[91], C. Alpigiani[139], Z. M. K. Alsolami[92], M. Alvarez Estevez[100], A. Alvarez Fernandez[101], M. Alves Cardoso[56], M. G. Alviggi[72a,72b], M. Aly[102], Y. Amaral Coutinho[83b], A. Ambler[105], C. Amelung[36], M. Amerl[102], C. G. Ames[110], D. Amidei[107], K. J. Amirie[156], S. P. Amor Dos Santos[131a], K. R. Amos[164], S. An[84], V. Ananiev[126], C. Anastopoulos[140], T. Andeen[11], J. K. Anders[36], S. Y. Andrean[47a,47b], A. Andreazza[71a,71b], S. Angelidakis[9], A. Angerami[41,aa], A. V. Anisenkov[37], A. Annovi[74a], C. Antel[56], E. Antipov[146], M. Antonelli[53], F. Anulli[75a], M. Aoki[84], T. Aoki[154], M. A. Aparo[147], L. Aperio Bella[48], C. Appelt[18], A. Apyan[26], S. J. Arbiol Val[87], C. Arcangeletti[53], A. T. H. Arce[51], E. Arena[93], J-F. Arguin[109], S. Argyropoulos[54], J.-H. Arling[48], O. Arnaez[4], H. Arnold[115], G. Artoni[75a,75b], H. Asada[112], K. Asai[119], S. Asai[154], N. A. Asbah[36], R. A. Ashby Pickering[168], K. Assamagan[29], R. Astalos[28a], K. S. V. Astrand[99], S. Atashi[160], R. J. Atkin[33a], M. Atkinson[163], H. Atmani[35f], P. A. Atmasiddha[129], K. Augsten[133], S. Auricchio[72a,72b], A. D. Auriol[20], V. A. Austrup[102], G. Avolio[36], K. Axiotis[56], G. Azuelos[109,ae], D. Babal[28b], H. Bachacou[136], K. Bachas[153,o], A. Bachiu[34], F. Backman[47a,47b], A. Badea[39], T. M. Baer[107], P. Bagnaia[75a,75b], M. Bahmani[18], D. Bahner[54], K. Bai[124], J. T. Baines[135], L. Baines[95], O. K. Baker[173], E. Bakos[15], D. Bakshi Gupta[8], V. Balakrishnan[121], R. Balasubramanian[115], E. M. Baldin[37], P. Balek[86a], E. Ballabene[23a,23b], F. Balli[136], L. M. Baltes[63a], W. K. Balunas[32], J. Balz[101], I. Bamwidhi[117b], E. Banas[87], M. Bandieramonte[130], A. Bandyopadhyay[24], S. Bansal[24], L. Barak[152], M. Barakat[48], E. L. Barberio[106], D. Barberis[57a,57b], M. Barbero[103], M. Z. Barel[115], K. N. Barends[33a], T. Barillari[111], M-S. Barisits[36], T. Barklow[144], P. Baron[123], D. A. Baron Moreno[102], A. Baroncelli[62a], G. Barone[29], A. J. Barr[127], J. D. Barr[97], F. Barreiro[100], J. Barreiro Guimarães da Costa[14a], U. Barron[152], M. G. Barros Teixeira[131a], S. Barsov[37], F. Bartels[63a], R. Bartoldus[144], A. E. Barton[92], P. Bartos[28a], A. Basan[101], M. Baselga[49], A. Bassalat[66,b], M. J. Basso[157a], R. Bate[165], R. L. Bates[59], S. Batlamous[100], B. Batool[142], M. Battaglia[137], D. Battulga[18], M. Bauce[75a,75b], M. Bauer[36], P. Bauer[24], L. T. Bazzano Hurrell[30], J. B. Beacham[51], T. Beau[128], J. Y. Beaucamp[91], P. H. Beauchemin[159], P. Bechtle[24], H. P. Beck[19,n], K. Becker[168], A. J. Beddall[82], V. A. Bednyakov[38], C. P. Bee[146], L. J. Beemster[15], T. A. Beermann[36], M. Begalli[83d], M. Begel[29], A. Behera[146], J. K. Behr[48], J. F. Beirer[36], F. Beisiegel[24], M. Belfkir[117b], G. Bella[152], L. Bellagamba[23b], A. Bellerive[34], P. Bellos[20], K. Beloborodov[37], D. Benchekroun[35a], F. Bendebba[35a], Y. Benhammou[152], K. C. Benkendorfer[61], L. Beresford[48], M. Beretta[53], E. Bergeaas Kuutmann[162], N. Berger[4], B. Bergmann[133], J. Beringer[17a], G. Bernardi[5], C. Bernius[144], F. U. Bernlochner[24], F. Bernon[36,103], A. Berrocal Guardia[13], T. Berry[96], P. Berta[134], A. Berthold[50], S. Bethke[111], A. Betti[75a,75b], A. J. Bevan[95], N. K. Bhalla[54], M. Bhamjee[33c], S. Bhatta[146], D. S. Bhattacharya[167], P. Bhattarai[144], K. D. Bhide[54], V. S. Bhopatkar[122], R. M. Bianchi[130], G. Bianco[23a,23b],

O. Biebel[110], R. Bielski[124], M. Biglietti[77a], C. S. Billingsley[44], M. Bindi[55], A. Bingul[21b], C. Bini[75a,75b], A. Biondini[93], C. J. Birch-sykes[102], G. A. Bird[32], M. Birman[170], M. Biros[134], S. Biryukov[147], T. Bisanz[49], E. Bisceglie[43a,43b], J. P. Biswal[135], D. Biswas[142], I. Bloch[48], A. Blue[59], U. Blumenschein[95], J. Blumenthal[101], V. S. Bobrovnikov[37], M. Boehler[54], B. Boehm[167], D. Bogavac[36], A. G. Bogdanchikov[37], C. Bohm[47a], V. Boisvert[96], P. Bokan[36], T. Bold[86a], M. Bomben[5], M. Bona[95], M. Boonekamp[136], C. D. Booth[96], A. G. Borbély[59], I. S. Bordulev[37], H. M. Borecka-Bielska[109], G. Borissov[92], D. Bortoletto[127], D. Boscherini[23b], M. Bosman[13], J. D. Bossio Sola[36], K. Bouaouda[35a], N. Bouchhar[164], L. Boudet[4], J. Boudreau[130], E. V. Bouhova-Thacker[92], D. Boumediene[40], R. Bouquet[57a,57b], A. Boveia[120], J. Boyd[36], D. Boye[29], I. R. Boyko[38], L. Bozianu[56], J. Bracinik[20], N. Brahimi[4], G. Brandt[172], O. Brandt[32], F. Braren[48], B. Brau[104], J. E. Brau[124], R. Brener[170], L. Brenner[115], R. Brenner[162], S. Bressler[170], D. Britton[59], D. Britzger[111], I. Brock[24], R. Brock[108], G. Brooijmans[41], E. Brost[29], L. M. Brown[166], L. E. Bruce[61], T. L. Bruckler[127], P. A. Bruckman de Renstrom[87], B. Brüers[48], A. Bruni[23b], G. Bruni[23b], M. Bruschi[23b], N. Bruscino[75a,75b], T. Buanes[16], Q. Buat[139], D. Buchin[111], A. G. Buckley[59], O. Bulekov[37], B. A. Bullard[144], S. Burdin[93], C. D. Burgard[49], A. M. Burger[36], B. Burghgrave[8], O. Burlayenko[54], J. T. P. Burr[32], J. C. Burzynski[143], E. L. Busch[41], V. Büscher[101], P. J. Bussey[59], J. M. Butler[25], C. M. Buttar[59], J. M. Butterworth[97], W. Buttinger[135], C. J. Buxo Vazquez[108], A. R. Buzykaev[37], S. Cabrera Urbán[164], L. Cadamuro[66], D. Caforio[58], H. Cai[130], Y. Cai[14a,14e], Y. Cai[14c], V. M. M. Cairo[36], O. Cakir[3a], N. Calace[36], P. Calafiura[17a], G. Calderini[128], P. Calfayan[68], G. Callea[59], L. P. Caloba[83b], D. Calvet[40], S. Calvet[40], M. Calvetti[74a,74b], R. Camacho Toro[128], S. Camarda[36], D. Camarero Munoz[26], P. Camarri[76a,76b], M. T. Camerlingo[72a,72b], D. Cameron[36], C. Camincher[166], M. Campanelli[97], A. Camplani[42], V. Canale[72a,72b], A. C. Canbay[3a], E. Canonero[96], J. Cantero[164], Y. Cao[163], F. Capocasa[26], M. Capua[43a,43b], A. Carbone[71a,71b], R. Cardarelli[76a], J. C. J. Cardenas[8], G. Carducci[43a,43b], T. Carli[36], G. Carlino[72a], J. I. Carlotto[13], B. T. Carlson[130,p], E. M. Carlson[157a,166], J. Carmignani[93], L. Carminati[71a,71b], A. Carnelli[136], M. Carnesale[75a,75b], S. Caron[114], E. Carquin[138f], S. Carrá[71a], G. Carratta[23a,23b], A. M. Carroll[124], T. M. Carter[52], M. P. Casado[13,h], M. Caspar[48], F. L. Castillo[4], L. Castillo Garcia[13], V. Castillo Gimenez[164], N. F. Castro[131a,131e], A. Catinaccio[36], J. R. Catmore[126], T. Cavaliere[4], V. Cavaliere[29], N. Cavalli[23a,23b], Y. C. Cekmecelioglu[48], E. Celebi[21a], S. Cella[36], F. Celli[127], M. S. Centonze[70a,70b], V. Cepaitis[56], K. Cerny[123], A. S. Cerqueira[83a], A. Cerri[147], L. Cerrito[76a,76b], F. Cerutti[17a], B. Cervato[142], A. Cervelli[23b], G. Cesarini[53], S. A. Cetin[82], D. Chakraborty[116], J. Chan[17a], W. Y. Chan[154], J. D. Chapman[32], E. Chapon[136], B. Chargeishvili[150b], D. G. Charlton[20], M. Chatterjee[19], C. Chauhan[134], Y. Che[14c], S. Chekanov[6], S. V. Chekulaev[157a], G. A. Chelkov[38,a], A. Chen[107], B. Chen[152], B. Chen[166], H. Chen[14c], H. Chen[29], J. Chen[62c], J. Chen[143], M. Chen[127], S. Chen[154], S. J. Chen[14c], X. Chen[62c,136], X. Chen[14b,ad], Y. Chen[62a], C. L. Cheng[171], H. C. Cheng[64a], S. Cheong[144], A. Cheplakov[38], E. Cheremushkina[48], E. Cherepanova[115], R. Cherkaoui El Moursli[35e], E. Cheu[7], K. Cheung[65], L. Chevalier[136], V. Chiarella[53], G. Chiarelli[74a], N. Chiedde[103], G. Chiodini[70a], A. S. Chisholm[20], A. Chitan[27b], M. Chitishvili[164], M. V. Chizhov[38,q], K. Choi[11], Y. Chou[139], E. Y. S. Chow[114], K. L. Chu[170], M. C. Chu[64a], X. Chu[14a,14e], J. Chudoba[132], J. J. Chwastowski[87], D. Cieri[111], K. M. Ciesla[86a], V. Cindro[94], A. Ciocio[17a], F. Cirotto[72a,72b], Z. H. Citron[170], M. Citterio[71a], D. A. Ciubotaru[27b], A. Clark[56], P. J. Clark[52], C. Clarry[156], J. M. Clavijo Columbie[48], S. E. Clawson[48], C. Clement[47a,47b], J. Clercx[48], Y. Coadou[103], M. Cobal[69a,69c], A. Coccaro[57b], R. F. Coelho Barrue[131a], R. Coelho Lopes De Sa[104], S. Coelli[71a], B. Cole[41], J. Collot[60], P. Conde Muiño[131a,131g], M. P. Connell[33c], S. H. Connell[33c], E. I. Conroy[127], F. Conventi[72a,af], H. G. Cooke[20], A. M. Cooper-Sarkar[127], F. A. Corchia[23a,23b], A. Cordeiro Oudot Choi[128], L. D. Corpe[40], M. Corradi[75a,75b], F. Corriveau[105,w], A. Cortes-Gonzalez[18], M. J. Costa[164], F. Costanza[4], D. Costanzo[140], B. M. Cote[120], J. Couthures[4], G. Cowan[96], K. Cranmer[171], D. Cremonini[23a,23b], S. Crépé-Renaudin[60], F. Crescioli[128], M. Cristinziani[142], M. Cristoforetti[78a,78b], V. Croft[115], J. E. Crosby[122], G. Crosetti[43a,43b], A. Cueto[100], Z. Cui[7], W. R. Cunningham[59], F. Curcio[164], J. R. Curran[52], P. Czodrowski[36], M. M. Czurylo[36], M. J. Da Cunha Sargedas De Sousa[57a,57b], J. V. Da Fonseca Pinto[83b], C. Da Via[102], W. Dabrowski[86a], T. Dado[49], S. Dahbi[149], T. Dai[107], D. Dal Santo[19], C. Dallapiccola[104], M. Dam[42], G. D'amen[29], V. D'Amico[110], J. Damp[101], J. R. Dandoy[34], D. Dannheim[36], M. Danninger[143], V. Dao[36], G. Darbo[57b], S. J. Das[29,ag], F. Dattola[48], S. D'Auria[71a,71b], A. D'Avanzo[72a,72b], C. David[33a], T. Davidek[134], I. Dawson[95], H. A. Day-hall[133], K. De[8], R. De Asmundis[72a], N. De Biase[48], S. De Castro[23a,23b], N. De Groot[114], P. de Jong[115], H. De la Torre[116], A. De Maria[14c], A. De Salvo[75a], U. De Sanctis[76a,76b], F. De Santis[70a,70b], A. De Santo[147], J. B. De Vivie De Regie[60], D. V. Dedovich[38], J. Degens[93], A. M. Deiana[44],

F. Del Corso[23a,23b], J. Del Peso[100], F. Del Rio[63a], L. Delagrange[128], F. Deliot[136], C. M. Delitzsch[49], M. Della Pietra[72a,72b], D. Della Volpe[56], A. Dell'Acqua[36], L. Dell'Asta[71a,71b], M. Delmastro[4], P. A. Delsart[60], S. Demers[173], M. Demichev[38], S. P. Denisov[37], L. D'Eramo[40], D. Derendarz[87], F. Derue[128], P. Dervan[93], K. Desch[24], C. Deutsch[24], F. A. Di Bello[57a,57b], A. Di Ciaccio[76a,76b], L. Di Ciaccio[4], A. Di Domenico[75a,75b], C. Di Donato[72a,72b], A. Di Girolamo[36], G. Di Gregorio[36], A. Di Luca[78a,78b], B. Di Micco[77a,77b], R. Di Nardo[77a,77b], M. Diamantopoulou[34], F. A. Dias[115], T. Dias Do Vale[143], M. A. Diaz[138a,138b], F. G. Diaz Capriles[24], M. Didenko[164], E. B. Diehl[107], S. Díez Cornell[48], C. Diez Pardos[142], C. Dimitriadi[24,162], A. Dimitrievska[20], J. Dingfelder[24], I-M. Dinu[27b], S. J. Dittmeier[63b], F. Dittus[36], M. Divisek[134], F. Djama[103], T. Djobava[150b], C. Doglioni[99,102], A. Dohnalova[28a], J. Dolejsi[134], Z. Dolezal[134], K. Domijan[86a], K. M. Dona[39], M. Donadelli[83c], B. Dong[108], J. Donini[40], A. D'Onofrio[72a,72b], M. D'Onofrio[93], J. Dopke[135], A. Doria[72a], N. Dos Santos Fernandes[131a], P. Dougan[102], M. T. Dova[91], A. T. Doyle[59], M. A. Draguet[127], E. Dreyer[170], I. Drivas-koulouris[10], M. Drnevich[118], M. Drozdova[56], D. Du[62a], T. A. du Pree[115], F. Dubinin[37], M. Dubovsky[28a], E. Duchovni[170], G. Duckeck[110], O. A. Ducu[27b], D. Duda[52], A. Dudarev[36], E. R. Duden[26], M. D'uffizi[102], L. Duflot[66], M. Dührssen[36], I. Duminica[27g], A. E. Dumitriu[27b], M. Dunford[63a], S. Dungs[49], K. Dunne[47a,47b], A. Duperrin[103], H. Duran Yildiz[3a], M. Düren[58], A. Durglishvili[150b], B. L. Dwyer[116], G. I. Dyckes[17a], M. Dyndal[86a], B. S. Dziedzic[36], Z. O. Earnshaw[147], G. H. Eberwein[127], B. Eckerova[28a], S. Eggebrecht[55], E. Egidio Purcino De Souza[128], L. F. Ehrke[56], G. Eigen[16], K. Einsweiler[17a], T. Ekelof[162], P. A. Ekman[99], S. El Farkh[35b], Y. El Ghazali[35b], H. El Jarrari[36], A. El Moussaouy[109], V. Ellajosyula[162], M. Ellert[162], F. Ellinghaus[172], N. Ellis[36], J. Elmsheuser[29], M. Elsawy[117a], M. Elsing[36], D. Emeliyanov[135], Y. Enari[154], I. Ene[17a], S. Epari[13], P. A. Erland[87], M. Errenst[172], M. Escalier[66], C. Escobar[164], E. Etzion[152], G. Evans[131a], H. Evans[68], L. S. Evans[96], A. Ezhilov[37], S. Ezzarqtouni[35a], F. Fabbri[23a,23b], L. Fabbri[23a,23b], G. Facini[97], V. Fadeyev[137], R. M. Fakhrutdinov[37], D. Fakoudis[101], S. Falciano[75a], L. F. Falda Ulhoa Coelho[36], F. Fallavollita[111], J. Faltova[134], C. Fan[163], Y. Fan[14a], Y. Fang[14a,14e], M. Fanti[71a,71b], M. Faraj[69a,69b], Z. Farazpay[98], A. Farbin[8], A. Farilla[77a], T. Farooque[108], S. M. Farrington[52], F. Fassi[35e], D. Fassouliotis[9], M. Faucci Giannelli[76a,76b], W. J. Fawcett[32], L. Fayard[66], P. Federic[134], P. Federicova[132], O. L. Fedin[37,a], M. Feickert[171], L. Feligioni[103], D. E. Fellers[124], C. Feng[62b], M. Feng[14b], Z. Feng[115], M. J. Fenton[160], L. Ferencz[48], R. A. M. Ferguson[92], S. I. Fernandez Luengo[138f], P. Fernandez Martinez[13], M. J. V. Fernoux[103], J. Ferrando[92], A. Ferrari[162], P. Ferrari[114,115], R. Ferrari[73a], D. Ferrere[56], C. Ferretti[107], F. Fiedler[101], P. Fiedler[133], A. Filipčič[94], E. K. Filmer[1], F. Filthaut[114], M. C. N. Fiolhais[131a,131c,c], L. Fiorini[164], W. C. Fisher[108], T. Fitschen[102], P. M. Fitzhugh[136], I. Fleck[142], P. Fleischmann[107], T. Flick[172], M. Flores[33d,ab], L. R. Flores Castillo[64a], L. Flores Sanz De Acedo[36], F. M. Follega[78a,78b], N. Fomin[16], J. H. Foo[156], A. Formica[136], A. C. Forti[102], E. Fortin[36], A. W. Fortman[17a], M. G. Foti[17a], L. Fountas[9,i], D. Fournier[66], H. Fox[92], P. Francavilla[74a,74b], S. Francescato[61], S. Franchellucci[56], M. Franchini[23a,23b], S. Franchino[63a], D. Francis[36], L. Franco[114], V. Franco Lima[36], L. Franconi[48], M. Franklin[61], G. Frattari[26], Y. Y. Frid[152], J. Friend[59], N. Fritzsche[50], A. Froch[54], D. Froidevaux[36], J. A. Frost[127], Y. Fu[62a], S. Fuenzalida Garrido[138f], M. Fujimoto[103], K. Y. Fung[64a], E. Furtado De Simas Filho[83e], M. Furukawa[154], J. Fuster[164], A. Gabrielli[23a,23b], A. Gabrielli[156], P. Gadow[36], G. Gagliardi[57a,57b], L. G. Gagnon[17a], S. Gaid[161], S. Galantzan[152], E. J. Gallas[127], B. J. Gallop[135], K. K. Gan[120], S. Ganguly[154], Y. Gao[52], F. M. Garay Walls[138a,138b], B. Garcia[29], C. García[164], A. Garcia Alonso[115], A. G. Garcia Caffaro[173], J. E. García Navarro[164], M. Garcia-Sciveres[17a], G. L. Gardner[129], R. W. Gardner[39], N. Garelli[159], D. Garg[80], R. B. Garg[144], J. M. Gargan[52], C. A. Garner[156], C. M. Garvey[33a], V. K. Gassmann[159], G. Gaudio[73a], V. Gautam[13], P. Gauzzi[75a,75b], I. L. Gavrilenko[37], A. Gavrilyuk[37], C. Gay[165], G. Gaycken[48], E. N. Gazis[10], A. A. Geanta[27b], C. M. Gee[137], A. Gekow[120], C. Gemme[57b], M. H. Genest[60], A. D. Gentry[113], S. George[96], W. F. George[20], T. Geralis[46], P. Gessinger-Befurt[36], M. E. Geyik[172], M. Ghani[168], K. Ghorbanian[95], A. Ghosal[142], A. Ghosh[160], A. Ghosh[7], B. Giacobbe[23b], S. Giagu[75a,75b], T. Giani[115], P. Giannetti[74a], A. Giannini[62a], S. M. Gibson[96], M. Gignac[137], D. T. Gil[86b], A. K. Gilbert[86a], B. J. Gilbert[41], D. Gillberg[34], G. Gilles[115], L. Ginabat[128], D. M. Gingrich[2,ae], M. P. Giordani[69a,69c], P. F. Giraud[136], G. Giugliarelli[69a,69c], D. Giugni[71a], F. Giuli[36], I. Gkialas[9,i], L. K. Gladilin[37], C. Glasman[100], G. R. Gledhill[124], G. Glemža[48], M. Glisic[124], I. Gnesi[43b,e], Y. Go[29], M. Goblirsch-Kolb[36], B. Gocke[49], D. Godin[109], B. Gokturk[21a], S. Goldfarb[106], T. Golling[56], M. G. D. Gololo[33g], D. Golubkov[37], J. P. Gombas[108], A. Gomes[131a,131b], G. Gomes Da Silva[142], A. J. Gomez Delegido[164], R. Gonçalo[131a], L. Gonella[20], A. Gongadze[150c], F. Gonnella[20], J. L. Gonski[144], R. Y. González Andana[52], S. González de la Hoz[164], R. Gonzalez Lopez[93],

C. Gonzalez Renteria[17a], M. V. Gonzalez Rodrigues[48], R. Gonzalez Suarez[162], S. Gonzalez-Sevilla[56], L. Goossens[36], B. Gorini[36], E. Gorini[70a,70b], A. Gorišek[94], T. C. Gosart[129], A. T. Goshaw[51], M. I. Gostkin[38], S. Goswami[122], C. A. Gottardo[36], S. A. Gotz[110], M. Gouighri[35b], V. Goumarre[48], A. G. Goussiou[139], N. Govender[33c], I. Grabowska-Bold[86a], K. Graham[34], E. Gramstad[126], S. Grancagnolo[70a,70b], C. M. Grant[1,136], P. M. Gravila[27f], F. G. Gravili[70a,70b], H. M. Gray[17a], M. Greco[70a,70b], C. Grefe[24], A. S. Grefsrud[16], I. M. Gregor[48], K. T. Greif[160], P. Grenier[144], S. G. Grewe[111], A. A. Grillo[137], K. Grimm[31], S. Grinstein[13,s], J.-F. Grivaz[66], E. Gross[170], J. Grosse-Knetter[55], J. C. Grundy[127], L. Guan[107], J. G. R. Guerrero Rojas[164], G. Guerrieri[69a,69c], F. Guescini[111], R. Gugel[101], J. A. M. Guhit[107], A. Guida[18], E. Guilloton[168], S. Guindon[36], F. Guo[14a,14e], J. Guo[62c], L. Guo[48], Y. Guo[107], R. Gupta[130], S. Gurbuz[24], S. S. Gurdasani[54], G. Gustavino[36], M. Guth[56], P. Gutierrez[121], L. F. Gutierrez Zagazeta[129], M. Gutsche[50], C. Gutschow[97], C. Gwenlan[127], C. B. Gwilliam[93], E. S. Haaland[126], A. Haas[118], M. Habedank[48], C. Haber[17a], H. K. Hadavand[8], A. Hadef[50], S. Hadzic[111], A. I. Hagan[92], J. J. Hahn[142], E. H. Haines[97], M. Haleem[167], J. Haley[122], J. J. Hall[140], G. D. Hallewell[103], L. Halser[19], K. Hamano[166], M. Hamer[24], G. N. Hamity[52], E. J. Hampshire[96], J. Han[62b], K. Han[62a], L. Han[14c], L. Han[62a], S. Han[17a], Y. F. Han[156], K. Hanagaki[84], M. Hance[137], D. A. Hangal[41], H. Hanif[143], M. D. Hank[129], J. B. Hansen[42], P. H. Hansen[42], K. Hara[158], D. Harada[56], T. Harenberg[172], S. Harkusha[37], M. L. Harris[104], Y. T. Harris[127], J. Harrison[13], N. M. Harrison[120], P. F. Harrison[168], N. M. Hartman[111], N. M. Hartmann[110], R. Z. Hasan[96,135], Y. Hasegawa[141], S. Hassan[16], R. Hauser[108], C. M. Hawkes[20], R. J. Hawkings[36], Y. Hayashi[154], S. Hayashida[112], D. Hayden[108], C. Hayes[107], R. L. Hayes[115], C. P. Hays[127], J. M. Hays[95], H. S. Hayward[93], F. He[62a], M. He[14a,14e], Y. He[155], Y. He[48], Y. He[97], N. B. Heatley[95], V. Hedberg[99], A. L. Heggelund[126], N. D. Hehir[95,*], C. Heidegger[54], K. K. Heidegger[54], W. D. Heidorn[81], J. Heilman[34], S. Heim[48], T. Heim[17a], J. G. Heinlein[129], J. J. Heinrich[124], L. Heinrich[111,ac], J. Hejbal[132], A. Held[171], S. Hellesund[16], C. M. Helling[165], S. Hellman[47a,47b], R. C. W. Henderson[92], L. Henkelmann[32], A. M. Henriques Correia[36], H. Herde[99], Y. Hernández Jiménez[146], L. M. Herrmann[24], T. Herrmann[50], G. Herten[54], R. Hertenberger[110], L. Hervas[36], M. E. Hesping[101], N. P. Hessey[157a], M. Hidaoui[35b], E. Hill[156], S. J. Hillier[20], J. R. Hinds[108], F. Hinterkeuser[24], M. Hirose[125], S. Hirose[158], D. Hirschbuehl[172], T. G. Hitchings[102], B. Hiti[94], J. Hobbs[146], R. Hobincu[27e], N. Hod[170], M. C. Hodgkinson[140], B. H. Hodkinson[127], A. Hoecker[36], D. D. Hofer[107], J. Hofer[48], T. Holm[24], M. Holzbock[111], L. B. A. H. Hommels[32], B. P. Honan[102], J. J. Hong[68], J. Hong[62c], T. M. Hong[130], B. H. Hooberman[163], W. H. Hopkins[6], M. C. Hoppesch[163], Y. Horii[112], S. Hou[149], A. S. Howard[94], J. Howarth[59], J. Hoya[6], M. Hrabovsky[123], A. Hrynevich[48], T. Hryn'ova[4], P. J. Hsu[65], S.-C. Hsu[139], T. Hsu[66], M. Hu[17a], Q. Hu[62a], S. Huang[64b], X. Huang[14a,14e], Y. Huang[140], Y. Huang[101], Y. Huang[14a], Z. Huang[102], Z. Hubacek[133], M. Huebner[24], F. Huegging[24], T. B. Huffman[127], C. A. Hugli[48], M. Huhtinen[36], S. K. Huiberts[16], R. Hulsken[105], N. Huseynov[12], J. Huston[108], J. Huth[61], R. Hyneman[144], G. Iacobucci[56], G. Iakovidis[29], L. Iconomidou-Fayard[66], J. P. Iddon[36], P. Iengo[72a,72b], R. Iguchi[154], T. Iizawa[127], Y. Ikegami[84], N. Ilic[156], H. Imam[35a], M. Ince Lezki[56], T. Ingebretsen Carlson[47a,47b], G. Introzzi[73a,73b], M. Iodice[77a], V. Ippolito[75a,75b], R. K. Irwin[93], M. Ishino[154], W. Islam[171], C. Issever[18,48], S. Istin[21a,ai], H. Ito[169], R. Iuppa[78a,78b], A. Ivina[170], J. M. Izen[45], V. Izzo[72a], P. Jacka[132], P. Jackson[1], C. S. Jagfeld[110], G. Jain[157a], P. Jain[48], K. Jakobs[54], T. Jakoubek[170], J. Jamieson[59], M. Javurkova[104], L. Jeanty[124], J. Jejelava[150a,z], P. Jenni[54,f], C. E. Jessiman[34], C. Jia[62b], J. Jia[146], X. Jia[61], X. Jia[14a,14e], Z. Jia[14c], C. Jiang[52], S. Jiggins[48], J. Jimenez Pena[13], S. Jin[14c], A. Jinaru[27b], O. Jinnouchi[155], P. Johansson[140], K. A. Johns[7], J. W. Johnson[137], D. M. Jones[147], E. Jones[48], P. Jones[32], R. W. L. Jones[92], T. J. Jones[93], H. L. Joos[36,55], R. Joshi[120], J. Jovicevic[15], X. Ju[17a], J. J. Junggeburth[104], T. Junkermann[63a], A. Juste Rozas[13,s], M. K. Juzek[87], S. Kabana[138e], A. Kaczmarska[87], M. Kado[111], H. Kagan[120], M. Kagan[144], A. Kahn[129], C. Kahra[101], T. Kaji[154], E. Kajomovitz[151], N. Kakati[170], I. Kalaitzidou[54], C. W. Kalderon[29], N. J. Kang[137], D. Kar[33g], K. Karava[127], M. J. Kareem[157b], E. Karentzos[54], O. Karkout[115], S. N. Karpov[38], Z. M. Karpova[38], V. Kartvelishvili[92], A. N. Karyukhin[37], E. Kasimi[153], J. Katzy[48], S. Kaur[34], K. Kawade[141], M. P. Kawale[121], C. Kawamoto[88], T. Kawamoto[62a], E. F. Kay[36], F. I. Kaya[159], S. Kazakos[108], V. F. Kazanin[37], Y. Ke[146], J. M. Keaveney[33a], R. Keeler[166], G. V. Kehris[61], J. S. Keller[34], A. S. Kelly[97], J. J. Kempster[147], P. D. Kennedy[101], O. Kepka[132], B. P. Kerridge[135], S. Kersten[172], B. P. Kerševan[94], L. Keszeghova[28a], S. Ketabchi Haghighat[156], R. A. Khan[130], A. Khanov[122], A. G. Kharlamov[37], T. Kharlamova[37], E. E. Khoda[139], M. Kholodenko[37], T. J. Khoo[18], G. Khoriauli[167], J. Khubua[150b], Y. A. R. Khwaira[128], B. Kibirige[33g], D. W. Kim[47a,47b], Y. K. Kim[39], N. Kimura[97], M. K. Kingston[55], A. Kirchhoff[55], C. Kirfel[24], F. Kirfel[24], J. Kirk[135],

A. E. Kiryunin[111], C. Kitsaki[10], O. Kivernyk[24], M. Klassen[159], C. Klein[34], L. Klein[167], M. H. Klein[44], S. B. Klein[56], U. Klein[93], P. Klimek[36], A. Klimentov[29], T. Klioutchnikova[36], P. Kluit[115], S. Kluth[111], E. Kneringer[79], T. M. Knight[156], A. Knue[49], R. Kobayashi[88], D. Kobylianskii[170], S. F. Koch[127], M. Kocian[144], P. Kodyš[134], D. M. Koeck[124], P. T. Koenig[24], T. Koffas[34], O. Kolay[50], I. Koletsou[4], T. Komarek[123], K. Köneke[54], A. X. Y. Kong[1], T. Kono[119], N. Konstantinidis[97], P. Kontaxakis[56], B. Konya[99], R. Kopeliansky[41], S. Koperny[86a], K. Korcyl[87], K. Kordas[153,d], A. Korn[97], S. Korn[55], I. Korolkov[13], N. Korotkova[37], B. Kortman[115], O. Kortner[111], S. Kortner[111], W. H. Kostecka[116], V. V. Kostyukhin[142], A. Kotsokechagia[136], A. Kotwal[51], A. Koulouris[36], A. Kourkoumeli-Charalampidi[73a,73b], C. Kourkoumelis[9], E. Kourlitis[111,ac], O. Kovanda[124], R. Kowalewski[166], W. Kozanecki[136], A. S. Kozhin[37], V. A. Kramarenko[37], G. Kramberger[94], P. Kramer[101], M. W. Krasny[128], A. Krasznahorkay[36], J. W. Kraus[172], J. A. Kremer[48], T. Kresse[50], J. Kretzschmar[93], K. Kreul[18], P. Krieger[156], S. Krishnamurthy[104], M. Krivos[134], K. Krizka[20], K. Kroeninger[49], H. Kroha[111], J. Kroll[132], J. Kroll[129], K. S. Krowpman[108], U. Kruchonak[38], H. Krüger[24], N. Krumnack[81], M. C. Kruse[51], O. Kuchinskaia[37], S. Kuday[3a], S. Kuehn[36], R. Kuesters[54], T. Kuhl[48], V. Kukhtin[38], Y. Kulchitsky[37,a], S. Kuleshov[138b,138d], M. Kumar[33g], N. Kumari[48], P. Kumari[157b], A. Kupco[132], T. Kupfer[49], A. Kupich[37], O. Kuprash[54], H. Kurashige[85], L. L. Kurchaninov[157a], O. Kurdysh[66], Y. A. Kurochkin[37], A. Kurova[37], M. Kuze[155], A. K. Kvam[104], J. Kvita[123], T. Kwan[105], N. G. Kyriacou[107], L. A. O. Laatu[103], C. Lacasta[164], F. Lacava[75a,75b], H. Lacker[18], D. Lacour[128], N. N. Lad[97], E. Ladygin[38], A. Lafarge[40], B. Laforge[128], T. Lagouri[173], F. Z. Lahbabi[35a], S. Lai[55], J. E. Lambert[166], S. Lammers[68], W. Lampl[7], C. Lampoudis[153,d], G. Lamprinoudis[101], A. N. Lancaster[116], E. Lançon[29], U. Landgraf[54], M. P. J. Landon[95], V. S. Lang[54], O. K. B. Langrekken[126], A. J. Lankford[160], F. Lanni[36], K. Lantzsch[24], A. Lanza[73a], J. F. Laporte[136], T. Lari[71a], F. Lasagni Manghi[23b], M. Lassnig[36], V. Latonova[132], A. Laudrain[101], A. Laurier[151], S. D. Lawlor[140], Z. Lawrence[102], R. Lazaridou[168], M. Lazzaroni[71a,71b], B. Le[102], E. M. Le Boulicaut[51], L. T. Le Pottier[17a], B. Leban[23a,23b], A. Lebedev[81], M. LeBlanc[102], F. Ledroit-Guillon[60], S. C. Lee[149], S. Lee[47a,47b], T. F. Lee[93], L. L. Leeuw[33c], H. P. Lefebvre[96], M. Lefebvre[166], C. Leggett[17a], G. Lehmann Miotto[36], M. Leigh[56], W. A. Leight[104], W. Leinonen[114], A. Leisos[153,r], M. A. L. Leite[83c], C. E. Leitgeb[18], R. Leitner[134], K. J. C. Leney[44], T. Lenz[24], S. Leone[74a], C. Leonidopoulos[52], A. Leopold[145], C. Leroy[109], R. Les[108], C. G. Lester[32], M. Levchenko[37], J. Levêque[4], L. J. Levinson[170], G. Levrini[23a,23b], M. P. Lewicki[87], C. Lewis[139], D. J. Lewis[4], A. Li[5], B. Li[62b], C. Li[62a], C-Q. Li[111], H. Li[62a], H. Li[62b], H. Li[14c], H. Li[14b], H. Li[62b], J. Li[62c], K. Li[139], L. Li[62c], M. Li[14a,14e], S. Li[14a,14e], S. Li[62c,62d], T. Li[5], X. Li[105], Z. Li[127], Z. Li[154], Z. Li[14a,14e], S. Liang[14a,14e], Z. Liang[14a], M. Liberatore[136], B. Liberti[76a], K. Lie[64c], J. Lieber Marin[83e], H. Lien[68], H. Lin[107], K. Lin[108], R. E. Lindley[7], J. H. Lindon[2], E. Lipeles[129], A. Lipniacka[16], A. Lister[165], J. D. Little[4], B. Liu[14a], B. X. Liu[14d], D. Liu[62c,62d], E. H. L. Liu[20], J. B. Liu[62a], J. K. K. Liu[32], K. Liu[62d], K. Liu[62c,62d], M. Liu[62a], M. Y. Liu[62a], P. Liu[14a], Q. Liu[62c,62d,139], X. Liu[62a], X. Liu[62b], Y. Liu[14d,14e], Y. L. Liu[62b], Y. W. Liu[62a], J. Llorente Merino[143], S. L. Lloyd[95], E. M. Lobodzinska[48], P. Loch[7], T. Lohse[18], K. Lohwasser[140], E. Loiacono[48], M. Lokajicek[132,*], J. D. Lomas[20], J. D. Long[163], I. Longarini[160], R. Longo[163], I. Lopez Paz[67], A. Lopez Solis[48], N. Lorenzo Martinez[4], A. M. Lory[110], M. Losada[117a], G. Löschcke Centeno[147], O. Loseva[37], X. Lou[47a,47b], X. Lou[14a,14e], A. Lounis[66], P. A. Love[92], G. Lu[14a,14e], M. Lu[66], S. Lu[129], Y. J. Lu[65], H. J. Lubatti[139], C. Luci[75a,75b], F. L. Lucio Alves[14c], F. Luehring[68], I. Luise[146], O. Lukianchuk[66], O. Lundberg[145], B. Lund-Jensen[145], N. A. Luongo[6], M. S. Lutz[36], A. B. Lux[25], D. Lynn[29], R. Lysak[132], E. Lytken[99], V. Lyubushkin[38], T. Lyubushkina[38], M. M. Lyukova[146], M. Firdaus M. Soberi[52], H. Ma[29], K. Ma[62a], L. L. Ma[62b], W. Ma[62a], Y. Ma[122], G. Maccarrone[53], J. C. MacDonald[101], P. C. Machado De Abreu Farias[83e], R. Madar[40], T. Madula[97], J. Maeda[85], T. Maeno[29], H. Maguire[140], V. Maiboroda[136], A. Maio[131a,131b,131d], K. Maj[86a], O. Majersky[48], S. Majewski[124], N. Makovec[66], V. Maksimovic[15], B. Malaescu[128], Pa. Malecki[87], V. P. Maleev[37], F. Malek[60,m], M. Mali[94], D. Malito[96], U. Mallik[80], S. Maltezos[10], S. Malyukov[38], J. Mamuzic[13], G. Mancini[53], M. N. Mancini[26], G. Manco[73a,73b], J. P. Mandalia[95], I. Mandić[94], L. Manhaes de Andrade Filho[83a], I. M. Maniatis[170], J. Manjarres Ramos[90], D. C. Mankad[170], A. Mann[110], S. Manzoni[36], L. Mao[62c], X. Mapekula[33c], A. Marantis[153,r], G. Marchiori[5], M. Marcisovsky[132], C. Marcon[71a], M. Marinescu[20], S. Marium[48], M. Marjanovic[121], A. Markhoos[54], M. Markovitch[66], E. J. Marshall[92], Z. Marshall[17a], S. Marti-Garcia[164], T. A. Martin[135], V. J. Martin[52], B. Martin dit Latour[16], L. Martinelli[75a,75b], M. Martinez[13,s], P. Martinez Agullo[164], V. I. Martinez Outschoorn[104], P. Martinez Suarez[13], S. Martin-Haugh[135], G. Martinovicova[134], V. S. Martoiu[27b], A. C. Martyniuk[97], A. Marzin[36], D. Mascione[78a,78b], L. Masetti[101], T. Mashimo[154], J. Masik[102],

A. L. Maslennikov[37], P. Massarotti[72a,72b], P. Mastrandrea[74a,74b], A. Mastroberardino[43a,43b], T. Masubuchi[154], T. Mathisen[162], J. Matousek[134], N. Matsuzawa[154], J. Maurer[27b], A. J. Maury[66], B. Maček[94], D. A. Maximov[37], A. E. May[102], R. Mazini[149], I. Maznas[116], M. Mazza[108], S. M. Mazza[137], E. Mazzeo[71a,71b], C. Mc Ginn[29], J. P. Mc Gowan[166], S. P. Mc Kee[107], C. C. McCracken[165], E. F. McDonald[106], A. E. McDougall[115], J. A. Mcfayden[147], R. P. McGovern[129], G. Mchedlidze[150b], R. P. Mckenzie[33g], T. C. Mclachlan[48], D. J. Mclaughlin[97], S. J. McMahon[135], C. M. Mcpartland[93], R. A. McPherson[166,w], S. Mehlhase[110], A. Mehta[93], D. Melini[164], B. R. Mellado Garcia[33g], A. H. Melo[55], F. Meloni[48], A. M. Mendes Jacques Da Costa[102], H. Y. Meng[156], L. Meng[92], S. Menke[111], M. Mentink[36], E. Meoni[43a,43b], G. Mercado[116], S. Merianos[153], C. Merlassino[69a,69c], L. Merola[72a,72b], C. Meroni[71a,71b], J. Metcalfe[6], A. S. Mete[6], E. Meuser[101], C. Meyer[68], J-P. Meyer[136], R. P. Middleton[135], L. Mijović[52], G. Mikenberg[170], M. Mikestikova[132], M. Mikuž[94], H. Mildner[101], A. Milic[36], D. W. Miller[39], E. H. Miller[144], L. S. Miller[34], A. Milov[170], D. A. Milstead[47a,47b], T. Min[14c], A. A. Minaenko[37], I. A. Minashvili[150b], L. Mince[59], A. I. Mincer[118], B. Mindur[86a], M. Mineev[38], Y. Mino[88], L. M. Mir[13], M. Miralles Lopez[59], M. Mironova[17a], A. Mishima[154], M. C. Missio[114], A. Mitra[168], V. A. Mitsou[164], Y. Mitsumori[112], O. Miu[156], P. S. Miyagawa[95], T. Mkrtchyan[63a], M. Mlinarevic[97], T. Mlinarevic[97], M. Mlynarikova[36], S. Mobius[19], P. Mogg[110], M. H. Mohamed Farook[113], A. F. Mohammed[14a,14e], S. Mohapatra[41], G. Mokgatitswane[33g], L. Moleri[170], B. Mondal[142], S. Mondal[133], K. Mönig[48], E. Monnier[103], L. Monsonis Romero[164], J. Montejo Berlingen[13], M. Montella[120], F. Montereali[77a,77b], F. Monticelli[91], S. Monzani[69a,69c], N. Morange[66], A. L. Moreira De Carvalho[48], M. Moreno Llácer[164], C. Moreno Martinez[56], P. Morettini[57b], S. Morgenstern[36], M. Morii[61], M. Morinaga[154], F. Morodei[75a,75b], L. Morvaj[36], P. Moschovakos[36], B. Moser[36], M. Mosidze[150b], T. Moskalets[54], P. Moskvitina[114], J. Moss[31,j], P. Moszkowicz[86a], A. Moussa[35d], E. J. W. Moyse[104], O. Mtintsilana[33g], S. Muanza[103], J. Mueller[130], D. Muenstermann[92], R. Müller[19], G. A. Mullier[162], A. J. Mullin[32], J. J. Mullin[129], D. P. Mungo[156], D. Munoz Perez[164], F. J. Munoz Sanchez[102], M. Murin[102], W. J. Murray[135,168], M. Muškinja[94], C. Mwewa[29], A. G. Myagkov[37,a], A. J. Myers[8], G. Myers[107], M. Myska[133], B. P. Nachman[17a], O. Nackenhorst[49], K. Nagai[127], K. Nagano[84], J. L. Nagle[29,ag], E. Nagy[103], A. M. Nairz[36], Y. Nakahama[84], K. Nakamura[84], K. Nakkalil[5], H. Nanjo[125], E. A. Narayanan[113], I. Naryshkin[37], L. Nasella[71a,71b], M. Naseri[34], S. Nasri[117b], C. Nass[24], G. Navarro[22a], J. Navarro-Gonzalez[164], R. Nayak[152], A. Nayaz[18], P. Y. Nechaeva[37], S. Nechaeva[23a,23b], F. Nechansky[48], L. Nedic[127], T. J. Neep[20], A. Negri[73a,73b], M. Negrini[23b], C. Nellist[115], C. Nelson[105], K. Nelson[107], S. Nemecek[132], M. Nessi[36,g], M. S. Neubauer[163], F. Neuhaus[101], J. Neundorf[48], P. R. Newman[20], C. W. Ng[130], Y. W. Y. Ng[48], B. Ngair[117a], H. D. N. Nguyen[109], R. B. Nickerson[127], R. Nicolaidou[136], J. Nielsen[137], M. Niemeyer[55], J. Niermann[55], N. Nikiforou[36], V. Nikolaenko[37,a], I. Nikolic-Audit[128], K. Nikolopoulos[20], P. Nilsson[29], I. Ninca[48], G. Ninio[152], A. Nisati[75a], N. Nishu[2], R. Nisius[111], J-E. Nitschke[50], E. K. Nkadimeng[33g], T. Nobe[154], T. Nommensen[148], M. B. Norfolk[140], R. R. B. Norisam[97], B. J. Norman[34], M. Noury[35a], J. Novak[94], T. Novak[94], L. Novotny[133], R. Novotny[113], L. Nozka[123], K. Ntekas[160], N. M. J. Nunes De Moura Junior[83b], J. Ocariz[128], A. Ochi[85], I. Ochoa[131a], S. Oerdek[48,t], J. T. Offermann[39], A. Ogrodnik[134], A. Oh[102], C. C. Ohm[145], H. Oide[84], R. Oishi[154], M. L. Ojeda[48], Y. Okumura[154], L. F. Oleiro Seabra[131a], S. A. Olivares Pino[138d], G. Oliveira Correa[13], D. Oliveira Damazio[29], D. Oliveira Goncalves[83a], J. L. Oliver[160], Ö. O. Öncel[54], A. P. O'Neill[19], A. Onofre[131a,131e], P. U. E. Onyisi[11], M. J. Oreglia[39], G. E. Orellana[91], D. Orestano[77a,77b], N. Orlando[13], R. S. Orr[156], V. O'Shea[59], L. M. Osojnak[129], R. Ospanov[62a], G. Otero y Garzon[30], H. Otono[89], P. S. Ott[63a], G. J. Ottino[17a], M. Ouchrif[35d], F. Ould-Saada[126], T. Ovsiannikova[139], M. Owen[59], R. E. Owen[135], V. E. Ozcan[21a], F. Ozturk[87], N. Ozturk[8], S. Ozturk[82], H. A. Pacey[127], A. Pacheco Pages[13], C. Padilla Aranda[13], G. Padovano[75a,75b], S. Pagan Griso[17a], G. Palacino[68], A. Palazzo[70a,70b], J. Pampel[24], J. Pan[173], T. Pan[64a], D. K. Panchal[11], C. E. Pandini[115], J. G. Panduro Vazquez[135], H. D. Pandya[1], H. Pang[14b], P. Pani[48], G. Panizzo[69a,69c], L. Panwar[128], L. Paolozzi[56], S. Parajuli[163], A. Paramonov[6], C. Paraskevopoulos[53], D. Paredes Hernandez[64b], A. Pareti[73a,73b], K. R. Park[41], T. H. Park[156], M. A. Parker[32], F. Parodi[57a,57b], E. W. Parrish[116], V. A. Parrish[52], J. A. Parsons[41], U. Parzefall[54], B. Pascual Dias[109], L. Pascual Dominguez[100], E. Pasqualucci[75a], S. Passaggio[57b], F. Pastore[96], P. Patel[87], U. M. Patel[51], J. R. Pater[102], T. Pauly[36], C. I. Pazos[159], J. Pearkes[144], M. Pedersen[126], R. Pedro[131a], S. V. Peleganchuk[37], O. Penc[36], E. A. Pender[52], G. D. Penn[173], K. E. Penski[110], M. Penzin[37], B. S. Peralva[83d], A. P. Pereira Peixoto[139], L. Pereira Sanchez[144], D. V. Perepelitsa[29,ag], E. Perez Codina[157a], M. Perganti[10], H. Pernegger[36], S. Perrella[75a,75b], O. Perrin[40], K. Peters[48], R. F. Y. Peters[102], B. A. Petersen[36], T. C. Petersen[42], E. Petit[103], V. Petousis[133],

C. Petridou[153,d], T. Petru[134], A. Petrukhin[142], M. Pettee[17a], N. E. Pettersson[36], A. Petukhov[37], K. Petukhova[134], R. Pezoa[138f], L. Pezzotti[36], G. Pezzullo[173], T. M. Pham[171], T. Pham[106], P. W. Phillips[135], G. Piacquadio[146], E. Pianori[17a], F. Piazza[124], R. Piegaia[30], D. Pietreanu[27b], A. D. Pilkington[102], M. Pinamonti[69a,69c], J. L. Pinfold[2], B. C. Pinheiro Pereira[131a], A. E. Pinto Pinoargote[136], L. Pintucci[69a,69c], K. M. Piper[147], A. Pirttikoski[56], D. A. Pizzi[34], L. Pizzimento[64b], A. Pizzini[115], M.-A. Pleier[29], V. Pleskot[134], E. Plotnikova[38], G. Poddar[95], R. Poettgen[99], L. Poggioli[128], I. Pokharel[55], S. Polacek[134], G. Polesello[73a], A. Poley[143,157a], A. Polini[23b], C. S. Pollard[168], Z. B. Pollock[120], E. Pompa Pacchi[75a,75b], N. I. Pond[97], D. Ponomarenko[114], L. Pontecorvo[36], S. Popa[27a], G. A. Popeneciu[27d], A. Poreba[36], D. M. Portillo Quintero[157a], S. Pospisil[133], M. A. Postill[140], P. Postolache[27c], K. Potamianos[168], P. A. Potepa[86a], I. N. Potrap[38], C. J. Potter[32], H. Potti[1], J. Poveda[164], M. E. Pozo Astigarraga[36], A. Prades Ibanez[164], J. Pretel[54], D. Price[102], M. Primavera[70a], M. A. Principe Martin[100], R. Privara[123], T. Procter[59], M. L. Proffitt[139], N. Proklova[129], K. Prokofiev[64c], G. Proto[111], J. Proudfoot[6], M. Przybycien[86a], W. W. Przygoda[86b], A. Psallidas[46], J. E. Puddefoot[140], D. Pudzha[37], D. Pyatiizbyantseva[37], J. Qian[107], D. Qichen[102], Y. Qin[13], T. Qiu[52], A. Quadt[55], M. Queitsch-Maitland[102], G. Quetant[56], R. P. Quinn[165], G. Rabanal Bolanos[61], D. Rafanoharana[54], F. Raffaeli[76a,76b], F. Ragusa[71a,71b], J. L. Rainbolt[39], J. A. Raine[56], S. Rajagopalan[29], E. Ramakoti[37], I. A. Ramirez-Berend[34], K. Ran[48,14e], N. P. Rapheeha[33g], H. Rasheed[27b], V. Raskina[128], D. F. Rassloff[63a], A. Rastogi[17a], S. Rave[101], B. Ravina[55], I. Ravinovich[170], M. Raymond[36], A. L. Read[126], N. P. Readioff[140], D. M. Rebuzzi[73a,73b], G. Redlinger[29], A. S. Reed[111], K. Reeves[26], J. A. Reidelsturz[172], D. Reikher[152], A. Rej[49], C. Rembser[36], M. Renda[27b], M. B. Rendel[111], F. Renner[48], A. G. Rennie[160], A. L. Rescia[48], S. Resconi[71a], M. Ressegotti[57a,57b], S. Rettie[36], J. G. Reyes Rivera[108], E. Reynolds[17a], O. L. Rezanova[37], P. Reznicek[134], H. Riani[35d], N. Ribaric[92], E. Ricci[78a,78b], R. Richter[111], S. Richter[47a,47b], E. Richter-Was[86b], M. Ridel[128], S. Ridouani[35d], P. Rieck[118], P. Riedler[36], E. M. Riefel[47a,47b], J. O. Rieger[115], M. Rijssenbeek[146], M. Rimoldi[36], L. Rinaldi[23a,23b], T. T. Rinn[29], M. P. Rinnagel[110], G. Ripellino[162], I. Riu[13], J. C. Rivera Vergara[166], F. Rizatdinova[122], E. Rizvi[95], B. R. Roberts[17a], S. H. Robertson[105,w], D. Robinson[32], C. M. Robles Gajardo[138f], M. Robles Manzano[101], A. Robson[59], A. Rocchi[76a,76b], C. Roda[74a,74b], S. Rodriguez Bosca[36], Y. Rodriguez Garcia[22a], A. Rodriguez Rodriguez[54], A. M. Rodríguez Vera[116], S. Roe[36], J. T. Roemer[160], A. R. Roepe-Gier[137], J. Roggel[172], O. Røhne[126], R. A. Rojas[104], C. P. A. Roland[128], J. Roloff[29], A. Romaniouk[37], E. Romano[73a,73b], M. Romano[23b], A. C. Romero Hernandez[163], N. Rompotis[93], L. Roos[128], S. Rosati[75a], B. J. Rosser[39], E. Rossi[127], E. Rossi[72a,72b], L. P. Rossi[61], L. Rossini[54], R. Rosten[120], M. Rotaru[27b], B. Rottler[54], C. Rougier[90], D. Rousseau[66], D. Rousso[48], A. Roy[163], S. Roy-Garand[156], A. Rozanov[103], Z. M. A. Rozario[59], Y. Rozen[151], A. Rubio Jimenez[164], A. J. Ruby[93], V. H. Ruelas Rivera[18], T. A. Ruggeri[1], A. Ruggiero[127], A. Ruiz-Martinez[164], A. Rummler[36], Z. Rurikova[54], N. A. Rusakovich[38], H. L. Russell[166], G. Russo[75a,75b], J. P. Rutherfoord[7], S. Rutherford Colmenares[32], M. Rybar[134], E. B. Rye[126], A. Ryzhov[44], J. A. Sabater Iglesias[56], P. Sabatini[164], H.F.-W. Sadrozinski[137], F. Safai Tehrani[75a], B. Safarzadeh Samani[135], S. Saha[1], M. Sahinsoy[111], A. Saibel[164], M. Saimpert[136], M. Saito[154], T. Saito[154], A. Sala[71a,71b], D. Salamani[36], A. Salnikov[144], J. Salt[164], A. Salvador Salas[152], D. Salvatore[43a,43b], F. Salvatore[147], A. Salzburger[36], D. Sammel[54], E. Sampson[92], D. Sampsonidis[153,d], D. Sampsonidou[124], J. Sánchez[164], V. Sanchez Sebastian[164], H. Sandaker[126], C. O. Sander[48], J. A. Sandesara[104], M. Sandhoff[172], C. Sandoval[22b], L. Sanfilippo[63a], D. P. C. Sankey[135], T. Sano[88], A. Sansoni[53], L. Santi[75a,75b], C. Santoni[40], H. Santos[131a,131b], A. Santra[170], E. Sanzani[23a,23b], K. A. Saoucha[161], J. G. Saraiva[131a,131d], J. Sardain[7], O. Sasaki[84], K. Sato[158], C. Sauer[63b], E. Sauvan[4], P. Savard[156,ae], R. Sawada[154], C. Sawyer[135], L. Sawyer[98], C. Sbarra[23b], A. Sbrizzi[23a,23b], T. Scanlon[97], J. Schaarschmidt[139], U. Schäfer[101], A. C. Schaffer[44,66], D. Schaile[110], R. D. Schamberger[146], C. Scharf[18], M. M. Schefer[19], V. A. Schegelsky[37], D. Scheirich[134], M. Schernau[160], C. Scheulen[55], C. Schiavi[57a,57b], M. Schioppa[43a,43b], B. Schlag[144,l], K. E. Schleicher[54], S. Schlenker[36], J. Schmeing[172], M. A. Schmidt[172], K. Schmieden[101], C. Schmitt[101], N. Schmitt[101], S. Schmitt[48], L. Schoeffel[136], A. Schoening[63b], P. G. Scholer[34], E. Schopf[127], M. Schott[24], J. Schovancova[36], S. Schramm[56], T. Schroer[56], H-C. Schultz-Coulon[63a], M. Schumacher[54], B. A. Schumm[137], Ph. Schune[136], A. J. Schuy[139], H. R. Schwartz[137], A. Schwartzman[144], T. A. Schwarz[107], Ph. Schwemling[136], R. Schwienhorst[108], A. Sciandra[29], G. Sciolla[26], F. Scuri[74a], C. D. Sebastiani[93], K. Sedlaczek[116], S. C. Seidel[113], A. Seiden[137], B. D. Seidlitz[41], C. Seitz[48], J. M. Seixas[83b], G. Sekhniaidze[72a], L. Selem[60], N. Semprini-Cesari[23a,23b], D. Sengupta[56], V. Senthilkumar[164], L. Serin[66], M. Sessa[76a,76b], H. Severini[121], F. Sforza[57a,57b], A. Sfyrla[56], Q. Sha[14a], E. Shabalina[55], A. H. Shah[32], R. Shaheen[145], J. D. Shahinian[129],

D. Shaked Renous[170], L. Y. Shan[14a], M. Shapiro[17a], A. Sharma[36], A. S. Sharma[165], P. Sharma[80], P. B. Shatalov[37], K. Shaw[147], S. M. Shaw[102], Q. Shen[5,62c], D. J. Sheppard[143], P. Sherwood[97], L. Shi[97], X. Shi[14a], C. O. Shimmin[173], J. D. Shinner[96], I. P. J. Shipsey[127], S. Shirabe[89], M. Shiyakova[38,u], M. J. Shochet[39], J. Shojaii[106], D. R. Shope[126], B. Shrestha[121], S. Shrestha[120,ah], M. J. Shroff[166], P. Sicho[132], A. M. Sickles[163], E. Sideras Haddad[33g], A. C. Sidley[115], A. Sidoti[23b], F. Siegert[50], Dj. Sijacki[15], F. Sili[91], J. M. Silva[52], M. V. Silva Oliveira[29], S. B. Silverstein[47a], S. Simion[66], R. Simoniello[36], E. L. Simpson[102], H. Simpson[147], L. R. Simpson[107], N. D. Simpson[99], S. Simsek[82], S. Sindhu[55], P. Sinervo[156], S. Singh[156], S. Sinha[48], S. Sinha[102], M. Sioli[23a,23b], I. Siral[36], E. Sitnikova[48], J. Sjölin[47a,47b], A. Skaf[55], E. Skorda[20], P. Skubic[121], M. Slawinska[87], V. Smakhtin[170], B. H. Smart[135], S.Yu. Smirnov[37], Y. Smirnov[37], L. N. Smirnova[37,a], O. Smirnova[99], A. C. Smith[41], D. R. Smith[160], E. A. Smith[39], H. A. Smith[127], J. L. Smith[102], R. Smith[144], M. Smizanska[92], K. Smolek[133], A. A. Snesarev[37], S. R. Snider[156], H. L. Snoek[115], S. Snyder[29], R. Sobie[166,w], A. Soffer[152], C. A. Solans Sanchez[36], E.Yu. Soldatov[37], U. Soldevila[164], A. A. Solodkov[37], S. Solomon[26], A. Soloshenko[38], K. Solovieva[54], O. V. Solovyanov[40], P. Sommer[36], A. Sonay[13], W. Y. Song[157b], A. Sopczak[133], A. L. Sopio[97], F. Sopkova[28b], J. D. Sorenson[113], I. R. Sotarriva Alvarez[155], V. Sothilingam[63a], O. J. Soto Sandoval[138b,138c], S. Sottocornola[68], R. Soualah[161], Z. Soumaimi[35e], D. South[48], N. Soybelman[170], S. Spagnolo[70a,70b], M. Spalla[111], D. Sperlich[54], G. Spigo[36], S. Spinali[92], D. P. Spiteri[59], M. Spousta[134], E. J. Staats[34], R. Stamen[63a], A. Stampekis[20], M. Standke[24], E. Stanecka[87], W. Stanek-Maslouska[48], M. V. Stange[50], B. Stanislaus[17a], M. M. Stanitzki[48], B. Stapf[48], E. A. Starchenko[37], G. H. Stark[137], J. Stark[90], P. Staroba[132], P. Starovoitov[63a], S. Stärz[105], R. Staszewski[87], G. Stavropoulos[46], J. Steentoft[162], P. Steinberg[29], B. Stelzer[143,157a], H. J. Stelzer[130], O. Stelzer-Chilton[157a], H. Stenzel[58], T. J. Stevenson[147], G. A. Stewart[36], J. R. Stewart[122], M. C. Stockton[36], G. Stoicea[27b], M. Stolarski[131a], S. Stonjek[111], A. Straessner[50], J. Strandberg[145], S. Strandberg[47a,47b], M. Stratmann[172], M. Strauss[121], T. Strebler[103], P. Strizenec[28b], R. Ströhmer[167], D. M. Strom[124], R. Stroynowski[44], A. Strubig[47a,47b], S. A. Stucci[29], B. Stugu[16], J. Stupak[121], N. A. Styles[48], D. Su[144], S. Su[62a], W. Su[62d], X. Su[62a], D. Suchy[28a], K. Sugizaki[154], V. V. Sulin[37], M. J. Sullivan[93], D. M. S. Sultan[127], L. Sultanaliyeva[37], S. Sultansoy[3b], T. Sumida[88], S. Sun[107], S. Sun[171], O. Sunneborn Gudnadottir[162], N. Sur[103], M. R. Sutton[147], H. Suzuki[158], M. Svatos[132], M. Swiatlowski[157a], T. Swirski[167], I. Sykora[28a], M. Sykora[134], T. Sykora[134], D. Ta[101], K. Tackmann[48,t], A. Taffard[160], R. Tafirout[157a], J. S. Tafoya Vargas[66], Y. Takubo[84], M. Talby[103], A. A. Talyshev[37], K. C. Tam[64b], N. M. Tamir[152], A. Tanaka[154], J. Tanaka[154], R. Tanaka[66], M. Tanasini[146], Z. Tao[165], S. Tapia Araya[138f], S. Tapprogge[101], A. Tarek Abouelfadl Mohamed[108], S. Tarem[151], K. Tariq[14a], G. Tarna[27b], G. F. Tartarelli[71a], M. J. Tartarin[90], P. Tas[134], M. Tasevsky[132], E. Tassi[43a,43b], A. C. Tate[163], G. Tateno[154], Y. Tayalati[35e,v], G. N. Taylor[106], W. Taylor[157b], A. S. Tee[171], R. Teixeira De Lima[144], P. Teixeira-Dias[96], J. J. Teoh[156], K. Terashi[154], J. Terron[100], S. Terzo[13], M. Testa[53], R. J. Teuscher[156,w], A. Thaler[79], O. Theiner[56], N. Themistokleous[52], T. Theveneaux-Pelzer[103], O. Thielmann[172], D. W. Thomas[96], J. P. Thomas[20], E. A. Thompson[17a], P. D. Thompson[20], E. Thomson[129], R. E. Thornberry[44], C. Tian[62a], Y. Tian[55], V. Tikhomirov[37,a], Yu. A. Tikhonov[37], S. Timoshenko[37], D. Timoshyn[134], E. X. L. Ting[1], P. Tipton[173], A. Tishelman-Charny[29], S. H. Tlou[33g], K. Todome[155], S. Todorova-Nova[134], S. Todt[50], L. Toffolin[69a,69c], M. Togawa[84], J. Tojo[89], S. Tokár[28a], K. Tokushuku[84], O. Toldaiev[68], R. Tombs[32], M. Tomoto[84,112], L. Tompkins[144,l], K. W. Topolnicki[86b], E. Torrence[124], H. Torres[90], E. Torró Pastor[164], M. Toscani[30], C. Tosciri[39], M. Tost[11], D. R. Tovey[140], A. Traeet[16], I. S. Trandafir[27b], T. Trefzger[167], A. Tricoli[29], I. M. Trigger[157a], S. Trincaz-Duvoid[128], D. A. Trischuk[26], B. Trocmé[60], L. Truong[33c], M. Trzebinski[87], A. Trzupek[87], F. Tsai[146], M. Tsai[107], A. Tsiamis[153,d], P. V. Tsiareshka[37], S. Tsigaridas[157a], A. Tsirigotis[153,r], V. Tsiskaridze[156], E. G. Tskhadadze[150a], M. Tsopoulou[153], Y. Tsujikawa[88], I. I. Tsukerman[37], V. Tsulaia[17a], S. Tsuno[84], K. Tsuri[119], D. Tsybychev[146], Y. Tu[64b], A. Tudorache[27b], V. Tudorache[27b], A. N. Tuna[61], S. Turchikhin[57a,57b], I. Turk Cakir[3a], R. Turra[71a], T. Turtuvshin[38,x], P. M. Tuts[41], S. Tzamarias[153,d], E. Tzovara[101], F. Ukegawa[158], P. A. Ulloa Poblete[138b,138c], E. N. Umaka[29], G. Unal[36], A. Undrus[29], G. Unel[160], J. Urban[28b], P. Urrejola[138a], G. Usai[8], R. Ushioda[155], M. Usman[109], Z. Uysal[82], V. Vacek[133], B. Vachon[105], T. Vafeiadis[36], A. Vaitkus[97], C. Valderanis[110], E. Valdes Santurio[47a,47b], M. Valente[157a], S. Valentinetti[23a,23b], A. Valero[164], E. Valiente Moreno[164], A. Vallier[90], J. A. Valls Ferrer[164], D. R. Van Arneman[115], T. R. Van Daalen[139], A. Van Der Graaf[49], P. Van Gemmeren[6], M. Van Rijnbach[36], S. Van Stroud[97], I. Van Vulpen[115], P. Vana[134], M. Vanadia[76a,76b], W. Vandelli[36], E. R. Vandewall[122], D. Vannicola[152], L. Vannoli[53], R. Vari[75a], E. W. Varnes[7], C. Varni[17b], T. Varol[149], D. Varouchas[66],

L. Varriale[164], K. E. Varvell[148], M. E. Vasile[27b], L. Vaslin[84], G. A. Vasquez[166], A. Vasyukov[38], R. Vavricka[101], T. Vazquez Schroeder[36], J. Veatch[31], V. Vecchio[102], M. J. Veen[104], I. Veliscek[29], L. M. Veloce[156], F. Veloso[131a,131c], S. Veneziano[75a], A. Ventura[70a,70b], S. Ventura Gonzalez[136], A. Verbytskyi[111], M. Verducci[74a,74b], C. Vergis[95], M. Verissimo De Araujo[83b], W. Verkerke[115], J. C. Vermeulen[115], C. Vernieri[144], M. Vessella[104], M. C. Vetterli[143,ae], A. Vgenopoulos[153,d], N. Viaux Maira[138f], T. Vickey[140], O. E. Vickey Boeriu[140], G. H. A. Viehhauser[127], L. Vigani[63b], M. Villa[23a,23b], M. Villaplana Perez[164], E. M. Villhauer[52], E. Vilucchi[53], M. G. Vincter[34], A. Visibile[115], C. Vittori[36], I. Vivarelli[23a,23b], E. Voevodina[111], F. Vogel[110], J. C. Voigt[50], P. Vokac[133], Yu. Volkotrub[86b], J. Von Ahnen[48], E. Von Toerne[24], B. Vormwald[36], V. Vorobel[134], K. Vorobev[37], M. Vos[164], K. Voss[142], M. Vozak[115], L. Vozdecky[121], N. Vranjes[15], M. Vranjes Milosavljevic[15], M. Vreeswijk[115], N. K. Vu[62c,62d], R. Vuillermet[36], O. Vujinovic[101], I. Vukotic[39], S. Wada[158], C. Wagner[104], J. M. Wagner[17a], W. Wagner[172], S. Wahdan[172], H. Wahlberg[91], M. Wakida[112], J. Walder[135], R. Walker[110], W. Walkowiak[142], A. Wall[129], E. J. Wallin[99], T. Wamorkar[6], A. Z. Wang[137], C. Wang[101], C. Wang[11], H. Wang[17a], J. Wang[64c], R. Wang[61], R. Wang[6], S. M. Wang[149], S. Wang[62b], S. Wang[14a], T. Wang[62a], W. T. Wang[80], W. Wang[14a], X. Wang[14c], X. Wang[163], X. Wang[62c], Y. Wang[62d], Y. Wang[14c], Z. Wang[107], Z. Wang[51,62c,62d], Z. Wang[107], A. Warburton[105], R. J. Ward[20], N. Warrack[59], S. Waterhouse[96], A. T. Watson[20], H. Watson[59], M. F. Watson[20], E. Watton[59,135], G. Watts[139], B. M. Waugh[97], J. M. Webb[54], C. Weber[29], H. A. Weber[18], M. S. Weber[19], S. M. Weber[63a], C. Wei[62a], Y. Wei[54], A. R. Weidberg[127], E. J. Weik[118], J. Weingarten[49], C. Weiser[54], C. J. Wells[48], T. Wenaus[29], B. Wendland[49], T. Wengler[36], N. S. Wenke[111], N. Wermes[24], M. Wessels[63a], A. M. Wharton[92], A. S. White[61], A. White[8], M. J. White[1], D. Whiteson[160], L. Wickremasinghe[125], W. Wiedenmann[171], M. Wielers[135], C. Wiglesworth[42], D. J. Wilbern[121], H. G. Wilkens[36], J. J. H. Wilkinson[32], D. M. Williams[41], H. H. Williams[129], S. Williams[32], S. Willocq[104], B. J. Wilson[102], P. J. Windischhofer[39], F. I. Winkel[30], F. Winklmeier[124], B. T. Winter[54], J. K. Winter[102], M. Wittgen[144], M. Wobisch[98], T. Wojtkowski[60], Z. Wolffs[115], J. Wollrath[160], M. W. Wolter[87], H. Wolters[131a,131c], M. C. Wong[137], E. L. Woodward[41], S. D. Worm[48], B. K. Wosiek[87], K. W. Woźniak[87], S. Wozniewski[55], K. Wraight[59], C. Wu[20], M. Wu[14d], M. Wu[114], S. L. Wu[171], X. Wu[56], Y. Wu[62a], Z. Wu[4], J. Wuerzinger[111,ac], T. R. Wyatt[102], B. M. Wynne[52], S. Xella[42], L. Xia[14c], M. Xia[14b], J. Xiang[64c], M. Xie[62a], S. Xin[14a,14e], A. Xiong[124], J. Xiong[17a], D. Xu[14a], H. Xu[62a], L. Xu[62a], R. Xu[129], T. Xu[107], Y. Xu[14b], Z. Xu[52], Z. Xu[14c], B. Yabsley[148], S. Yacoob[33a], Y. Yamaguchi[155], E. Yamashita[154], H. Yamauchi[158], T. Yamazaki[17a], Y. Yamazaki[85], J. Yan[62c], S. Yan[59], Z. Yan[104], H. J. Yang[62c,62d], H. T. Yang[62a], S. Yang[62a], T. Yang[64c], X. Yang[36], X. Yang[14a], Y. Yang[44], Y. Yang[62a], Z. Yang[62a], W-M. Yao[17a], H. Ye[14c], H. Ye[55], J. Ye[14a], S. Ye[29], X. Ye[62a], Y. Yeh[97], I. Yeletskikh[38], B. Yeo[17b], M. R. Yexley[97], T. P. Yildirim[127], P. Yin[41], K. Yorita[169], S. Younas[27b], C. J. S. Young[36], C. Young[144], C. Yu[14a,14e], Y. Yu[62a], M. Yuan[107], R. Yuan[62c,62d], L. Yue[97], M. Zaazoua[62a], B. Zabinski[87], E. Zaid[52], Z. K. Zak[87], T. Zakareishvili[164], N. Zakharchuk[34], S. Zambito[56], J. A. Zamora Saa[138b,138d], J. Zang[154], D. Zanzi[54], O. Zaplatilek[133], C. Zeitnitz[172], H. Zeng[14a], J. C. Zeng[163], D. T. Zenger Jr[26], O. Zenin[37], T. Ženiš[28a], S. Zenz[95], S. Zerradi[35a], D. Zerwas[66], M. Zhai[14a,14e], D. F. Zhang[140], J. Zhang[62b], J. Zhang[6], K. Zhang[14a,14e], L. Zhang[62a], L. Zhang[14c], P. Zhang[14a,14e], R. Zhang[171], S. Zhang[107], S. Zhang[90], T. Zhang[154], X. Zhang[62c], X. Zhang[62b], Y. Zhang[62c], Y. Zhang[97], Y. Zhang[14c], Z. Zhang[17a], Z. Zhang[62b], Z. Zhang[66], H. Zhao[139], T. Zhao[62b], Y. Zhao[137], Z. Zhao[62a], Z. Zhao[62a], A. Zhemchugov[38], J. Zheng[14c], K. Zheng[163], X. Zheng[62a], Z. Zheng[144], D. Zhong[163], B. Zhou[107], H. Zhou[7], N. Zhou[62c], Y. Zhou[14b], Y. Zhou[14c], Y. Zhou[7], C. G. Zhu[62b], J. Zhu[107], X. Zhu[62d], Y. Zhu[62c], Y. Zhu[62a], X. Zhuang[14a], K. Zhukov[37], N. I. Zimine[38], J. Zinsser[63b], M. Ziolkowski[142], L. Živković[15], A. Zoccoli[23a,23b], K. Zoch[61], T. G. Zorbas[140], O. Zormpa[46], W. Zou[41], L. Zwalinski[36]

[1] Department of Physics, University of Adelaide, Adelaide, Australia
[2] Department of Physics, University of Alberta, Edmonton, AB, Canada
[3] [(a)]Department of Physics, Ankara University, Ankara, Turkey; [(b)]Division of Physics, TOBB University of Economics and Technology, Ankara, Turkey
[4] LAPP, Université Savoie Mont Blanc, CNRS/IN2P3, Annecy, France
[5] APC, Université Paris Cité, CNRS/IN2P3, Paris, France
[6] High Energy Physics Division, Argonne National Laboratory, Argonne, IL, USA
[7] Department of Physics, University of Arizona, Tucson, AZ, USA
[8] Department of Physics, University of Texas at Arlington, Arlington, TX, USA

[9] Physics Department, National and Kapodistrian University of Athens, Athens, Greece
[10] Physics Department, National Technical University of Athens, Zografou, Greece
[11] Department of Physics, University of Texas at Austin, Austin, TX, USA
[12] Institute of Physics, Azerbaijan Academy of Sciences, Baku, Azerbaijan
[13] Institut de Física d'Altes Energies (IFAE), Barcelona Institute of Science and Technology, Barcelona, Spain
[14] [(a)]Institute of High Energy Physics, Chinese Academy of Sciences, Beijing, China; [(b)]Physics Department, Tsinghua University, Beijing, China; [(c)]Department of Physics, Nanjing University, Nanjing, China; [(d)]School of Science, Shenzhen Campus of Sun Yat-sen University, Shenzhen, China; [(e)]University of Chinese Academy of Science (UCAS), Beijing, China
[15] Institute of Physics, University of Belgrade, Belgrade, Serbia
[16] Department for Physics and Technology, University of Bergen, Bergen, Norway
[17] [(a)]Physics Division, Lawrence Berkeley National Laboratory, Berkeley, CA, USA; [(b)]University of California, Berkeley, CA, USA
[18] Institut für Physik, Humboldt Universität zu Berlin, Berlin, Germany
[19] Albert Einstein Center for Fundamental Physics and Laboratory for High Energy Physics, University of Bern, Bern, Switzerland
[20] School of Physics and Astronomy, University of Birmingham, Birmingham, UK
[21] [(a)]Department of Physics, Bogazici University, Istanbul, Türkiye; [(b)]Department of Physics Engineering, Gaziantep University, Gaziantep, Türkiye; [(c)]Department of Physics, Istanbul University, Istanbul, Türkiye
[22] [(a)]Facultad de Ciencias y Centro de Investigaciónes, Universidad Antonio Nariño, Bogotá, Colombia; [(b)]Departamento de Física, Universidad Nacional de Colombia, Bogotá, Colombia
[23] [(a)]Dipartimento di Fisica e Astronomia A. Righi, Università di Bologna, Bologna, Italy; [(b)]INFN Sezione di Bologna, Bologna, Italy
[24] Physikalisches Institut, Universität Bonn, Bonn, Germany
[25] Department of Physics, Boston University, Boston, MA, USA
[26] Department of Physics, Brandeis University, Waltham, MA, USA
[27] [(a)]Transilvania University of Brasov, Brasov, Romania; [(b)]Horia Hulubei National Institute of Physics and Nuclear Engineering, Bucharest, Romania; [(c)]Department of Physics, Alexandru Ioan Cuza University of Iasi, Iasi, Romania; [(d)]Physics Department, National Institute for Research and Development of Isotopic and Molecular Technologies, Cluj-Napoca, Romania; [(e)]National University of Science and Technology Politechnica, Bucharest, Romania; [(f)]West University in Timisoara, Timisoara, Romania; [(g)]Faculty of Physics, University of Bucharest, Bucharest, Romania
[28] [(a)]Faculty of Mathematics, Physics and Informatics, Comenius University, Bratislava, Slovak Republic; [(b)]Department of Subnuclear Physics, Institute of Experimental Physics of the Slovak Academy of Sciences, Kosice, Slovak Republic
[29] Physics Department, Brookhaven National Laboratory, Upton, NY, USA
[30] Universidad de Buenos Aires, Facultad de Ciencias Exactas y Naturales, Departamento de Física, y CONICET, Instituto de Física de Buenos Aires (IFIBA), Buenos Aires, Argentina
[31] California State University, Los Angeles, CA, USA
[32] Cavendish Laboratory, University of Cambridge, Cambridge, UK
[33] [(a)]Department of Physics, University of Cape Town, Cape Town, South Africa; [(b)]iThemba Labs, Western Cape, South Africa; [(c)]Department of Mechanical Engineering Science, University of Johannesburg, Johannesburg, South Africa; [(d)]National Institute of Physics, University of the Philippines, Diliman, Philippines; [(e)]Department of Physics, University of South Africa, Pretoria, South Africa; [(f)]University of Zululand, KwaDlangezwa, South Africa; [(g)]School of Physics, University of the Witwatersrand, Johannesburg, South Africa
[34] Department of Physics, Carleton University, Ottawa, ON, Canada
[35] [(a)]Faculté des Sciences Ain Chock, Université Hassan II de Casablanca, Casablanca, Morocco; [(b)]Faculté des Sciences, Université Ibn-Tofail, Kénitra, Morocco; [(c)]Faculté des Sciences Semlalia, Université Cadi Ayyad, LPHEA-Marrakech, Morocco; [(d)]LPMR, Faculté des Sciences, Université Mohamed Premier, Oujda, Morocco; [(e)]Faculté des sciences, Université Mohammed V, Rabat, Morocco; [(f)]Institute of Applied Physics, Mohammed VI Polytechnic University, Ben Guerir, Morocco
[36] CERN, Geneva, Switzerland
[37] Affiliated with an Institute Covered by a Cooperation Agreement with CERN, Geneva, Switzerland
[38] Affiliated with an international laboratory covered by a cooperation agreement with CERN, Geneva, Switzerland

[39] Enrico Fermi Institute, University of Chicago, Chicago, IL, USA
[40] LPC, Université Clermont Auvergne, CNRS/IN2P3, Clermont-Ferrand, France
[41] Nevis Laboratory, Columbia University, Irvington, NY, USA
[42] Niels Bohr Institute, University of Copenhagen, Copenhagen, Denmark
[43] [(a)]Dipartimento di Fisica, Università della Calabria, Rende, Italy; [(b)]INFN Gruppo Collegato di Cosenza, Laboratori Nazionali di Frascati, Frascati, Italy
[44] Physics Department, Southern Methodist University, Dallas, TX, USA
[45] Physics Department, University of Texas at Dallas, Richardson, TX, USA
[46] National Centre for Scientific Research "Demokritos", Agia Paraskevi, Greece
[47] [(a)]Department of Physics, Stockholm University, Stockholm, Sweden; [(b)]Oskar Klein Centre, Stockholm, Sweden
[48] Deutsches Elektronen-Synchrotron DESY, Hamburg and Zeuthen, Germany
[49] Fakultät Physik , Technische Universität Dortmund, Dortmund, Germany
[50] Institut für Kern- und Teilchenphysik, Technische Universität Dresden, Dresden, Germany
[51] Department of Physics, Duke University, Durham, NC, USA
[52] SUPA-School of Physics and Astronomy, University of Edinburgh, Edinburgh, UK
[53] INFN e Laboratori Nazionali di Frascati, Frascati, Italy
[54] Physikalisches Institut, Albert-Ludwigs-Universität Freiburg, Freiburg, Germany
[55] II. Physikalisches Institut, Georg-August-Universität Göttingen, Göttingen, Germany
[56] Département de Physique Nucléaire et Corpusculaire, Université de Genève, Geneva, Switzerland
[57] [(a)]Dipartimento di Fisica, Università di Genova, Genoa, Italy; [(b)]INFN Sezione di Genova, Genoa, Italy
[58] II. Physikalisches Institut, Justus-Liebig-Universität Giessen, Giessen, Germany
[59] SUPA-School of Physics and Astronomy, University of Glasgow, Glasgow, UK
[60] LPSC, Université Grenoble Alpes, CNRS/IN2P3, Grenoble INP, Grenoble, France
[61] Laboratory for Particle Physics and Cosmology, Harvard University, Cambridge, MA, USA
[62] [(a)]Department of Modern Physics and State Key Laboratory of Particle Detection and Electronics, University of Science and Technology of China, Hefei, China; [(b)]Institute of Frontier and Interdisciplinary Science and Key Laboratory of Particle Physics and Particle Irradiation (MOE), Shandong University, Qingdao, China; [(c)]School of Physics and Astronomy, Shanghai Jiao Tong University, Key Laboratory for Particle Astrophysics and Cosmology (MOE), SKLPPC, Shanghai, China; [(d)]Tsung-Dao Lee Institute, Shanghai, China; [(e)]School of Physics and Microelectronics, Zhengzhou University, Zhengzhou, China
[63] [(a)]Kirchhoff-Institut für Physik, Ruprecht-Karls-Universität Heidelberg, Heidelberg, Germany; [(b)]Physikalisches Institut, Ruprecht-Karls-Universität Heidelberg, Heidelberg, Germany
[64] [(a)]Department of Physics, Chinese University of Hong Kong, Shatin, N.T., Hong Kong, China; [(b)]Department of Physics, University of Hong Kong, Hong Kong, China; [(c)]Department of Physics and Institute for Advanced Study, Hong Kong University of Science and Technology, Clear Water Bay, Kowloon, Hong Kong, China
[65] Department of Physics, National Tsing Hua University, Hsinchu, Taiwan
[66] IJCLab, Université Paris-Saclay, CNRS/IN2P3, 91405 Orsay, France
[67] Centro Nacional de Microelectrónica (IMB-CNM-CSIC), Barcelona, Spain
[68] Department of Physics, Indiana University, Bloomington, IN, USA
[69] [(a)]INFN Gruppo Collegato di Udine, Sezione di Trieste, Udine, Italy; [(b)]ICTP, Trieste, Italy; [(c)]Dipartimento Politecnico di Ingegneria e Architettura, Università di Udine, Udine, Italy
[70] [(a)]INFN Sezione di Lecce, Lecce, Italy; [(b)]Dipartimento di Matematica e Fisica, Università del Salento, Lecce, Italy
[71] [(a)]INFN Sezione di Milano, Milan, Italy; [(b)]Dipartimento di Fisica, Università di Milano, Milan, Italy
[72] [(a)]INFN Sezione di Napoli, Naples, Italy; [(b)]Dipartimento di Fisica, Università di Napoli, Naples, Italy
[73] [(a)]INFN Sezione di Pavia, Pavia, Italy; [(b)]Dipartimento di Fisica, Università di Pavia, Pavia, Italy
[74] [(a)]INFN Sezione di Pisa, Pisa, Italy; [(b)]Dipartimento di Fisica E. Fermi, Università di Pisa, Pisa, Italy
[75] [(a)]INFN Sezione di Roma, Rome, Italy; [(b)]Dipartimento di Fisica, Sapienza Università di Roma, Rome, Italy
[76] [(a)]INFN Sezione di Roma Tor Vergata, Rome, Italy; [(b)]Dipartimento di Fisica, Università di Roma Tor Vergata, Rome, Italy
[77] [(a)]INFN Sezione di Roma Tre, Rome, Italy; [(b)]Dipartimento di Matematica e Fisica, Università Roma Tre, Rome, Italy
[78] [(a)]INFN-TIFPA, Povo, Italy; [(b)]Università degli Studi di Trento, Trento, Italy
[79] Department of Astro and Particle Physics, Universität Innsbruck, Innsbruck, Austria
[80] University of Iowa, Iowa City, IA, USA

[81] Department of Physics and Astronomy, Iowa State University, Ames, IA, USA
[82] Istinye University, Sariyer, Istanbul, Türkiye
[83] [(a)]Departamento de Engenharia Elétrica, Universidade Federal de Juiz de Fora (UFJF), Juiz de Fora, Brazil; [(b)]Universidade Federal do Rio De Janeiro COPPE/EE/IF, Rio de Janeiro, Brazil; [(c)]Instituto de Física, Universidade de São Paulo, São Paulo, Brazil; [(d)]Rio de Janeiro State University, Rio de Janeiro, Brazil; [(e)]Federal University of Bahia, Bahia, Brazil
[84] KEK, High Energy Accelerator Research Organization, Tsukuba, Japan
[85] Graduate School of Science, Kobe University, Kobe, Japan
[86] [(a)]Faculty of Physics and Applied Computer Science, AGH University of Krakow, Krakow, Poland; [(b)]Marian Smoluchowski Institute of Physics, Jagiellonian University, Krakow, Poland
[87] Institute of Nuclear Physics Polish Academy of Sciences, Krakow, Poland
[88] Faculty of Science, Kyoto University, Kyoto, Japan
[89] Research Center for Advanced Particle Physics and Department of Physics, Kyushu University, Fukuoka , Japan
[90] L2IT, Université de Toulouse, CNRS/IN2P3, UPS, Toulouse, France
[91] Instituto de Física La Plata, Universidad Nacional de La Plata and CONICET, La Plata, Argentina
[92] Physics Department, Lancaster University, Lancaster, UK
[93] Oliver Lodge Laboratory, University of Liverpool, Liverpool, UK
[94] Department of Experimental Particle Physics, Jožef Stefan Institute and Department of Physics, University of Ljubljana, Ljubljana, Slovenia
[95] School of Physics and Astronomy, Queen Mary University of London, London, UK
[96] Department of Physics, Royal Holloway University of London, Egham, UK
[97] Department of Physics and Astronomy, University College London, London, UK
[98] Louisiana Tech University, Ruston, LA, USA
[99] Fysiska institutionen, Lunds universitet, Lund, Sweden
[100] Departamento de Física Teorica C-15 and CIAFF, Universidad Autónoma de Madrid, Madrid, Spain
[101] Institut für Physik, Universität Mainz, Mainz, Germany
[102] School of Physics and Astronomy, University of Manchester, Manchester, UK
[103] CPPM, Aix-Marseille Université, CNRS/IN2P3, Marseille, France
[104] Department of Physics, University of Massachusetts, Amherst, MA, USA
[105] Department of Physics, McGill University, Montreal, QC, Canada
[106] School of Physics, University of Melbourne, Victoria, Australia
[107] Department of Physics, University of Michigan, Ann Arbor, MI, USA
[108] Department of Physics and Astronomy, Michigan State University, East Lansing, MI, USA
[109] Group of Particle Physics, University of Montreal, Montreal, QC, Canada
[110] Fakultät für Physik, Ludwig-Maximilians-Universität München, Munich, Germany
[111] Max-Planck-Institut für Physik (Werner-Heisenberg-Institut), Munich, Germany
[112] Graduate School of Science and Kobayashi-Maskawa Institute, Nagoya University, Nagoya, Japan
[113] Department of Physics and Astronomy, University of New Mexico, Albuquerque, NM, USA
[114] Institute for Mathematics, Astrophysics and Particle Physics, Radboud University/Nikhef, Nijmegen, The Netherlands
[115] Nikhef National Institute for Subatomic Physics and University of Amsterdam, Amsterdam, The Netherlands
[116] Department of Physics, Northern Illinois University, DeKalb, IL, USA
[117] [(a)]New York University Abu Dhabi, Abu Dhabi, United Arab Emirates; [(b)]United Arab Emirates University, Al Ain, United Arab Emirates
[118] Department of Physics, New York University, New York, NY, USA
[119] Ochanomizu University, Otsuka, Bunkyo-ku, Tokyo, Japan
[120] Ohio State University, Columbus, OH, USA
[121] Homer L. Dodge Department of Physics and Astronomy, University of Oklahoma, Norman, OK, USA
[122] Department of Physics, Oklahoma State University, Stillwater, OK, USA
[123] Palacký University, Joint Laboratory of Optics, Olomouc, Czech Republic
[124] Institute for Fundamental Science, University of Oregon, Eugene, OR, USA
[125] Graduate School of Science, Osaka University, Osaka, Japan
[126] Department of Physics, University of Oslo, Oslo, Norway
[127] Department of Physics, Oxford University, Oxford, UK

[128] LPNHE, Sorbonne Université, Université Paris Cité, CNRS/IN2P3, Paris, France
[129] Department of Physics, University of Pennsylvania, Philadelphia, PA, USA
[130] Department of Physics and Astronomy, University of Pittsburgh, Pittsburgh, PA, USA
[131] [(a)]Laboratório de Instrumentação e Física Experimental de Partículas-LIP, Lisbon, Portugal; [(b)]Departamento de Física, Faculdade de Ciências, Universidade de Lisboa, Lisbon, Portugal; [(c)]Departamento de Física, Universidade de Coimbra, Coimbra, Portugal; [(d)]Centro de Física Nuclear da Universidade de Lisboa, Lisbon, Portugal; [(e)]Departamento de Física, Universidade do Minho, Braga, Portugal; [(f)]Departamento de Física Teórica y del Cosmos, Universidad de Granada, Granada, Spain; [(g)]Departamento de Física, Instituto Superior Técnico, Universidade de Lisboa, Lisbon, Portugal
[132] Institute of Physics of the Czech Academy of Sciences, Prague, Czech Republic
[133] Czech Technical University in Prague, Prague, Czech Republic
[134] Faculty of Mathematics and Physics, Charles University, Prague, Czech Republic
[135] Particle Physics Department, Rutherford Appleton Laboratory, Didcot, UK
[136] IRFU, CEA, Université Paris-Saclay, Gif-sur-Yvette, France
[137] Santa Cruz Institute for Particle Physics, University of California Santa Cruz, Santa Cruz, CA, USA
[138] [(a)]Departamento de Física, Pontificia Universidad Católica de Chile, Santiago, Chile; [(b)]Millennium Institute for Subatomic physics at high energy frontier (SAPHIR), Santiago, Chile; [(c)]Instituto de Investigación Multidisciplinario en Ciencia y Tecnología y Departamento de Física, Universidad de La Serena, La Serena, Chile; [(d)]Department of Physics, Universidad Andres Bello, Santiago, Chile; [(e)]Instituto de Alta Investigación, Universidad de Tarapacá, Arica, Chile; [(f)]Departamento de Física, Universidad Técnica Federico Santa María, Valparaíso, Chile
[139] Department of Physics, University of Washington, Seattle, WA, USA
[140] Department of Physics and Astronomy, University of Sheffield, Sheffield, UK
[141] Department of Physics, Shinshu University, Nagano, Japan
[142] Department Physik, Universität Siegen, Siegen, Germany
[143] Department of Physics, Simon Fraser University, Burnaby, BC, Canada
[144] SLAC National Accelerator Laboratory, Stanford, CA, USA
[145] Department of Physics, Royal Institute of Technology, Stockholm, Sweden
[146] Departments of Physics and Astronomy, Stony Brook University, Stony Brook, NY, USA
[147] Department of Physics and Astronomy, University of Sussex, Brighton, UK
[148] School of Physics, University of Sydney, Sydney, Australia
[149] Institute of Physics, Academia Sinica, Taipei, Taiwan
[150] [(a)]E. Andronikashvili Institute of Physics, Iv. Javakhishvili Tbilisi State University, Tbilisi, Georgia; [(b)]High Energy Physics Institute, Tbilisi State University, Tbilisi, Georgia; [(c)]University of Georgia, Tbilisi, Georgia
[151] Department of Physics, Technion, Israel Institute of Technology, Haifa, Israel
[152] Raymond and Beverly Sackler School of Physics and Astronomy, Tel Aviv University, Tel Aviv, Israel
[153] Department of Physics, Aristotle University of Thessaloniki, Thessaloniki, Greece
[154] International Center for Elementary Particle Physics and Department of Physics, University of Tokyo, Tokyo, Japan
[155] Department of Physics, Tokyo Institute of Technology, Tokyo, Japan
[156] Department of Physics, University of Toronto, Toronto, ON, Canada
[157] [(a)]TRIUMF, Vancouver, BC, Canada; [(b)]Department of Physics and Astronomy, York University, Toronto, ON, Canada
[158] Division of Physics and Tomonaga Center for the History of the Universe, Faculty of Pure and Applied Sciences, University of Tsukuba, Tsukuba, Japan
[159] Department of Physics and Astronomy, Tufts University, Medford, MA, USA
[160] Department of Physics and Astronomy, University of California Irvine, Irvine, CA, USA
[161] University of Sharjah, Sharjah, United Arab Emirates
[162] Department of Physics and Astronomy, University of Uppsala, Uppsala, Sweden
[163] Department of Physics, University of Illinois, Urbana, IL, USA
[164] Instituto de Física Corpuscular (IFIC), Centro Mixto Universidad de Valencia-CSIC, Valencia, Spain
[165] Department of Physics, University of British Columbia, Vancouver, BC, Canada
[166] Department of Physics and Astronomy, University of Victoria, Victoria, BC, Canada
[167] Fakultät für Physik und Astronomie, Julius-Maximilians-Universität Würzburg, Würzburg, Germany
[168] Department of Physics, University of Warwick, Coventry, UK
[169] Waseda University, Tokyo, Japan
[170] Department of Particle Physics and Astrophysics, Weizmann Institute of Science, Rehovot, Israel

[171] Department of Physics, University of Wisconsin, Madison, WI, USA
[172] Fakultät für Mathematik und Naturwissenschaften, Fachgruppe Physik, Bergische Universität Wuppertal, Wuppertal, Germany
[173] Department of Physics, Yale University, New Haven, CT, USA

[a] Also Affiliated with an Institute Covered by a Cooperation Agreement with CERN, Geneva, Switzerland
[b] Also at An-Najah National University, Nablus, Palestine
[c] Also at Borough of Manhattan Community College, City University of New York, New York, NY, USA
[d] Also at Center for Interdisciplinary Research and Innovation (CIRI-AUTH), Thessaloniki, Greece
[e] Also at Centro Studi e Ricerche Enrico Fermi, Rome, Italy
[f] Also at CERN, Geneva, Switzerland
[g] Also at Département de Physique Nucléaire et Corpusculaire, Université de Genève, Geneva, Switzerland
[h] Also at Departament de Fisica de la Universitat Autonoma de Barcelona, Barcelona, Spain
[i] Also at Department of Financial and Management Engineering, University of the Aegean, Chios, Greece
[j] Also at Department of Physics, California State University, Sacramento, USA
[k] Also at Department of Physics, King's College London, London, UK
[l] Also at Department of Physics, Stanford University, Stanford, CA, USA
[m] Also at Department of Physics, Stellenbosch University, South Africa
[n] Also at Department of Physics, University of Fribourg, Fribourg, Switzerland
[o] Also at Department of Physics, University of Thessaly, Volos, Greece
[p] Also at Department of Physics, Westmont College, Santa Barbara, USA
[q] Also at Faculty of Physics, Sofia University, 'St. Kliment Ohridski', Sofia, Bulgaria
[r] Also at Hellenic Open University, Patras, Greece
[s] Also at Institucio Catalana de Recerca i Estudis Avancats, ICREA, Barcelona, Spain
[t] Also at Institut für Experimentalphysik, Universität Hamburg, Hamburg, Germany
[u] Also at Institute for Nuclear Research and Nuclear Energy (INRNE) of the Bulgarian Academy of Sciences, Sofia, Bulgaria
[v] Also at Institute of Applied Physics, Mohammed VI Polytechnic University, Ben Guerir, Morocco
[w] Also at Institute of Particle Physics (IPP), Victoria, Canada
[x] Also at Institute of Physics and Technology, Mongolian Academy of Sciences, Ulaanbaatar, Mongolia
[y] Also at Institute of Physics, Azerbaijan Academy of Sciences, Baku, Azerbaijan
[z] Also at Institute of Theoretical Physics, Ilia State University, Tbilisi, Georgia
[aa] Also at Lawrence Livermore National Laboratory, Livermore, USA
[ab] Also at National Institute of Physics, University of the Philippines, Diliman, Philippines
[ac] Also at Technical University of Munich, Munich, Germany
[ad] Also at The Collaborative Innovation Center of Quantum Matter (CICQM), Beijing, China
[ae] Also at TRIUMF, Vancouver, BC, Canada
[af] Also at Università di Napoli Parthenope, Naples, Italy
[ag] Also at Department of Physics, University of Colorado Boulder, Boulder, CO, USA
[ah] Also at Washington College, Chestertown, MD, USA
[ai] Also at Physics Department, Yeditepe University, Istanbul, Türkiye
* Deceased